Energy Conversion and Management: X 22 (2024) 100543

Contents lists available at ScienceDirect

Energy Conversion and Management: X

journal homepage: www.sciencedirect.com/journal/energy-conversion-and-management-x

Technical performance analysis of high-voltage battery-based photovoltaic water pumping systems

José-Ángel Garrido-Sarasol [a], Salvador Orts-Grau [a], María Gasque [b], Pablo González-Altozano [c], Ibán Balbastre-Peralta [c], Francisco-José Gimeno-Sales [a], Salvador Segui-Chilet [a,*]

[a] Instituto Interuniversitario de Investigación de Reconocimiento Molecular y Desarrollo Tecnológico (IDM), Universitat Politècnica de València, Valencia 46022, Spain
[b] Dpto. de Física Aplicada, Universitat Politècnica de València, Valencia 46022, Spain
[c] Dpto. de Ingeniería Rural y Agroalimentaria (DIRA), Universitat Politècnica de València, Valencia 46022, Spain

ARTICLE INFO

Keywords:
High-voltage lithium-ion battery storage solutions
Battery-based photovoltaic water pumping systems
Energy efficiency
Optimum operating point
SOC management
Performance ratio

ABSTRACT

Energy efficiency in photovoltaic systems is especially important when batteries are part of the system. Performance optimization includes the selection of the best efficiency point for each stage of the system, and the inclusion of devices that reduce energy losses when some elements of the system are not operating. This paper proposes improving battery-based photovoltaic pumping systems by using high-voltage lithium batteries, combined with the inclusion of IoT switches and the operation of the pumping system at its most efficient operating point. Experimental results of a system working with different irradiance profiles are included for an analysis of the main working parameters. These parameters demonstrate how the inclusion of IoT switches improves system efficiency and provides extra energy that can be used to pump additional water or for other purposes. A comparison of the results obtained with the estimates made for direct pumping shows that the battery-based solution yields an average increase of 10.85 % on a sunny day (with 5.29 PSH) and 16.37 % on a cloudy day (with 2.88 PSH). Some water is pumped on days with less than 2 PSH, while direct pumping is unable to pump on those very cloudy days.

1. Introduction

The sustainable management of water supply based on renewable resources is essential, especially in developing countries or areas with water scarcity [1]. It also contributes to achieving the Sustainable Development Goals set by the United Nations [2]. Water demand depends on the population supplied, usage and type of service, local weather, and seasonal variations, etc. [3]. Both water and energy demand usually increase when availability increases [4]. The World Health Organization recommends a typical water consumption per person of between 50 and 100 L/d [5], although in humanitarian emergencies this can decrease to 20 L/d or less, as reported in [6]. A minimum of 7.5 L per capita per day is recommended to meet the requirements of most people under most conditions [7]. Pumping systems are used for the extraction and supply of water. The technological solutions available for water pumping infrastructure are analyzed in [8,9]. Grid-connected, fuel-based, or battery-based water pumping systems (WPSs) can operate at rated conditions, while solar pumping progressively pumps the required water volume during daylight hours. Due to the different modes of operation of direct photovoltaic water pumping systems (DPVWPS) (only at nominal conditions for a short period at midday on sunny days), the time needed to pump a fixed volume of water is longer. Since the daily operating time in DPVWPS is limited by sunshine hours, the pumps chosen require more power than those used in pumping systems based on energy sources without variability or time limitations. The direct use of PV power without an energy storage solution, as proposed in [10–13], is unusual when DPVWPS is located in rural isolated areas or in humanitarian aid contexts, in which the installation has more purposes than mere irrigation. In these cases, the use of some type of energy buffer, such as an elevated tank for water storage or the inclusion of batteries in the system, is common since it becomes necessary, as evidenced in [1,14–16]. In some cases, solar tracking systems are used to improve the operation of solar self-consuming grid-connected installations, as they avoid investments in storage systems and provide more stable operation with fewer fluctuations in the variable speed drive (VSD) [17]. The low level of maintenance required by DPVWPS results in low operating costs when

* Corresponding author.
E-mail addresses: jogars11@upv.es (J.-Á. Garrido-Sarasol), sorts@upv.es (S. Orts-Grau), mgasque@fis.upv.es (M. Gasque), pgaltozano@agf.upv.es (P. González-Altozano), ibbalpe@agf.upv.es (I. Balbastre-Peralta), fjgimeno@upv.es (F.-J. Gimeno-Sales), ssegui@upv.es (S. Segui-Chilet).

https://doi.org/10.1016/j.ecmx.2024.100543
Received 22 December 2023; Received in revised form 29 January 2024; Accepted 30 January 2024
Available online 2 February 2024

Nomenclature

AC	Alternate current
AV	Average (subscript)
BMS	Battery management system
cha	Charge of the battery (subscript)
d	Day
DB	Database
DC	Direct current
dis	Discharge of the battery (subscript)
DOD	Depth of discharge
DOY	Day of year
DPVWPS	Direct photovoltaic water pumping system
E_{**}	Energy in **
EB	Energy balance
EPS	Emergency power supply
est	Estimation (subscript)
EV	Electric vehicle
f_{VSD}	Frequency of the three-phase voltages in the VSD output
g	Acceleration of gravity (9.81 m/s^2)
GI	Global irradiance (in W/m^2)
h	Hydraulic (subscript)
hyb	Hybrid (subscript related to the hybrid inverter)
I_{**}	Current in device ** or current in conditions **
LIB	Lithium-ion battery
max	Maximum (subscript)
min	Minimum (subscript)
min	Minute
MPPT	Maximum power point tracking
mp	Motor-pump (subscript)
P_{**}	Power in device ** or power in conditions **
PCU	Power converter unit (use for the combination of hybrid inverter plus VSD)
PF	Power factor
PF_m	Power factor of the motor installed in the motor-pump group
pk	Peak (subscript)
PR_{**}	Performance ratio in device ** (quotient of energies)
PSH	Peak sun hours (1 PSH = 1 kWh/m^2)
PV	Photovoltaic
PVWPS	Photovoltaic water pumping system
PVWPS + LIB	Photovoltaic water pumping system with storage in a lithium-ion battery
PVWPS + LIB(HV)	Photovoltaic water pumping system with storage in a high-voltage lithium-ion battery
Q	Flow rate
r^2	Coefficient of determination
SBEP	Solar best efficiency point
SD	Standard deviation
SDG	Sustainable development goal
SL-LIB	Second-life lithium-ion batteries
SOC	State of charge
SOH	State of health
TDH	Total dynamic head
thre	Threshold (subscript)
t_k	Recording interval
V_d	Total volume of water pumped in a day
V_{d^*}	Corrected total volume of water pumped in a day
V_{**}	Voltage in device ** or voltage in conditions **
VSD	Variable speed drive
WPS	Water pumping system
η_{**}	Efficiency in device ** (quotient of powers)
ρ	Density of water (1000 kg/m^3)

compared to fuel-based solutions [18]. A study presented in [19] compared three PVWPS schemes for irrigation with the same 44.4 kW_{pk} PV field (DPVWPS, with and without an elevated water tank, and a battery-based PVWPS), and concluded that the battery-based solution was more cost-effective than the scheme with water storage. From the simulations performed in HOMER, it was found that a large battery capacity of 144 kWh presented a variation of the battery state of charge (*SOC*) of between 40 % and 100 % in July (the month with the maximum water requirements). It was concluded in [9] that battery-based PVWPS were more economical than fuel-based water pumping systems due to the continuous increase in fuel costs.

The main problem found in [20,21] with the rated operation of the WPS was the performance ratio (PR) decrease relative to the solar best efficiency point (SBEP) of the DPVWPS as defined in [22]. This reduction in efficiency was unimportant in fuel-powered WPSs because the auxiliary generator was usually oversized with respect to the power requirements of the WPS [4]. However, in battery-based WPSs the operation at the SBEP represents an electrical energy saving that could be used for increasing the pumping time, or for other appliances and purposes. Improved battery performance, expected price reductions, and research on the optimization of battery-based solar pumping systems will soon enable the replacement of auxiliary generators with these hybrid solar systems in humanitarian emergencies (following the guidelines given in [2]).

The use of DPVWPS has become popular in developing regions without an available power grid. The high cost of fossil fuels has led to the conversion of conventional pumping systems into solar pumping systems, both for the supply of drinking water to people and animals and for irrigation, although often a hybrid WPS, including a diesel auxiliary generator, could be installed to ensure the supply and reduce the water shortage probability [23]. The importance of the topic is evidenced in the periodic reviews published on solar pumping in the last decade [24–34]. Problems when implanting DPVWPS in isolated communities were identified in [4,8], and [23], including a lack of dissemination of DPVWPS, the false perception of its high price, and the misconception that it is a complex technology. The use of PV-based WPS is one of the solutions for reducing long-term operational costs and the environmental impact of ensuring water supply for off-grid communities and refugees [35].

Although the use of second-life lithium-ion batteries (SL-LIB) in WPSs for irrigation in poor and depressed regions in India and Bangladesh was proposed in 2014 [36], very few experimental works are related to battery-based WPS. The electric vehicle (EV) market is quickly growing and so a major increase is expected in lithium-ion batteries (LIB) packs that cannot provide satisfactory performance to power EVs. The end of LIB automotive life is usually determined by a state-of-health (*SOH*) below 80 %, although this value is under study due to technological advances in LIB production and chemistries [37]. Although recycling and recovery are recommended and necessary options, the use of these SL-LIB packs in less-demanding applications is an interesting and promising alternative (with environmental benefits) that extend their use after reaching their end-of-life for EVs. Following this line of research, the economic and technological viability of SL-LIB applications was analyzed in [38]. An example of the use of SL-LIBs in an off-grid application was described in [39]. The hybrid mini-grid system used an AC coupling bus in which were connected two SMA Sunny Boy 5.0 PV inverters to manage the energy produced by the PV field of 10.58 kW_{pk} and a bidirectional inverter (SMA Sunny Island 8.0H) that managed the AC bus and the charging and discharging of the 44 V and 85 kWh SL-LIB.

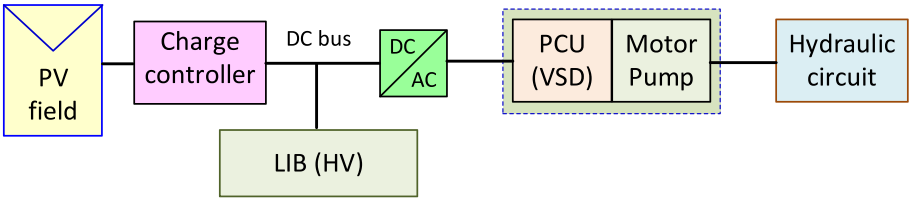

Fig. 1. Block diagram of a PV pumping system with the battery directly connected to the DC bus [32].

As described in [3], it is common to find a water pumping system in stand-alone PV installations with an existing battery bank that supplies energy to all the household electrical loads. In this situation, a water pumping system for irrigation and charging of portable devices could be considered as secondary applications (or diversion loads) that minimize the energy wastage in off-grid PV applications by 19 % to 45 % in accordance with [40]. The approach presented in [20,21] differed from the latter because the initial goal was to store and use surplus electrical energy lost by the DPVWPS during normal operation. Energy losses in DPVWPS, estimated in [23] at 28 % of the energy that can be produced by the PV field, were related to: threshold irradiance levels at sunrise (GI_{thre_start}) and sunset (GI_{thre_stop}) [41]; power curtailment in the central hours of sunny days due to the PV power exceeding the electric motor rated power [41]; improper tuning of the PID control of the VSD on days with variable irradiance [42]; start/stop cycles in days with variable sunshine; reduction in water demand; or cloudy days with little sunshine [21]. Oversizing the PV generator is a common way to ensure the water demand profile in remote areas, resulting in water storage tanks that are completely full at certain times of the day and the corresponding loss of PV power [18]. The surplus electrical energy that can be provided by the PV field could be used in other appliances to improve the long-term standard of living of the population settled around the DPVWPS location, such as in internally displaced people and Tier 0 refugee camps (regions without access to energy, according to [43]), as well as local communities living in off-grid areas, especially in developing countries [44]. This goal of harnessing surplus energy from photovoltaic pumping for use in domestic and community applications other than irrigation was already detailed in [36]. In this setting, photovoltaic water pumping systems including lithium-ion batteries (PVWPS + LIB facilities) can provide a basic level of electrification for remote off-grid areas while maintaining and guaranteeing water supply to the population, based on sustainable energies, as stated in the SDGs [2]. Some of the uses given to PV electricity were described in [45,46]. The level of access to electrical energy provided is between Tier 1 (solar lighting kits, with daily consumption per household greater than 12 Wh) and Tier 2 (standalone or home solar systems, with daily consumption per household greater than 200 Wh) as classified in [47]. This approach could offer humanitarian organizations sustainable and efficient solutions for covering basic energy needs in displacement settings with little investment, in a stage before the deployment of mini-grids, as analyzed in [4].

Experimental results presented in [36] were focused on the LIB behavior of a PVWPS + LIB facility with the following main characteristics: centrifugal pump suitable only for surface water lifting with a maximum suction head of 6.5 m; DC motor with 746 W and a maximum operating voltage of 60 V; LIB with a rated voltage of 51.8 V and 5.2 kWh at 80 % depth of discharge (*DOD*). The test had a duration of 3 h and 10 min, with a consumption of only 1.37 kWh (26.3 % of the total capacity). The LIB presented a very stable range of operation for the current and voltage that was better than expected for a lead-acid battery. The advantages of LIBs with respect to lead-acid batteries in renewable energy systems was pointed out since the previous decade [48–50]. A 5.2 kWp solar pumping system was simulated and compared with two identical electro-hydraulic systems with and without energy storage respectively [41]. The obtained results confirmed that the amount of water pumped increased by 33 % in case system equipped with energy storage. A solar water pumping system including a 12 V and 131Ah lead-acid battery backup was described in [51]. In this study, the 21 W_{pk} PV module provided all the energy needed for an automated system (approx. 60 Wh/day) that limited the diffusion of pollutants into a water stream. As will be seen in the next section, there is currently a trend towards higher voltage batteries to reduce the flow currents in the system, and this involves improvements in semiconductor components, cable cross-sections, etc.

In this contribution, the authors analyze a high-voltage lithium-ion battery-based PV pumping system (PVWPS + LIB(HV)) that includes IoT devices to optimize the energy use in the facility. By using the best operating point of the water pumping system, various efficiencies and performance ratios (PR) are obtained from the powers and energies in the different parts of the system. Operation of the battery-based solution is analyzed for different day profiles, and these results are compared with the estimations for the direct solution under the same irradiance profile. Changes in the monitoring system are described and the main problems found with the energy balance in the battery are detailed.

This study is within the frame of the project “Greening humanitarian responses through enhanced solar energy harvesting”, supported by the International Organization of Migration (IOM), with founding from the Bureau for Humanitarian Assistance – USAID, and the European Commission Humanitarian Aid & Civil Protection. The objectives of the project cover, in a first stage, the development of a multipurpose prototype of PVWPS + LIB(HV). A pilot pumping facility has been installed at the laboratory, being analyzed and characterized in the present paper with the intention of optimizing its operation. In a second stage of the project, the prototype will be implemented in some rural isolated communities with a view to water supply to population and facilitate utilization of surplus electrical energy.

These actions offer an innovative approach to support the shift to cleaner and more efficient energy solutions in the provision of water and electrical energy to vulnerable populations in humanitarian aid contexts, contributing therefore with SDGs attainment in developing countries. Specifically, the present study contributes to the achievement of Goal 6 (Ensure availability and sustainable management of water and sanitation for all), Goal 7 (Ensure access to affordable, reliable, sustainable and modern energy for all), Goal 11 (Make cities and human settlements inclusive, safe, resilient and sustainable), Goal 12 (Ensure sustainable consumption and production patterns), and Goal 17 (Strengthen the means of implementation and revitalize the Global Partnership for Sustainable Development).

The remainder of the article is organized as follows. Section 2 reviews the literature on the various alternatives for high-voltage battery-based water pumping. Section 3 summarizes the main features of the pumping facility used. Section 4 details the experimental tests performed and presents the key values for its optimum operating point (efficiencies and performance ratios), as well as the main issues related with *SOC* management. Section 5 presents the experimental results achieved for several days with various irradiance profiles, and considers the daily energy balance in the lithium-ion battery. Section 6 details the results obtained in the facility for the selected days and the averaged values for 20 days of operation. A comparison between the pumped volume obtained with the battery-based solution and estimations for direct pumping mode are also included. Section 7 summarizes the main

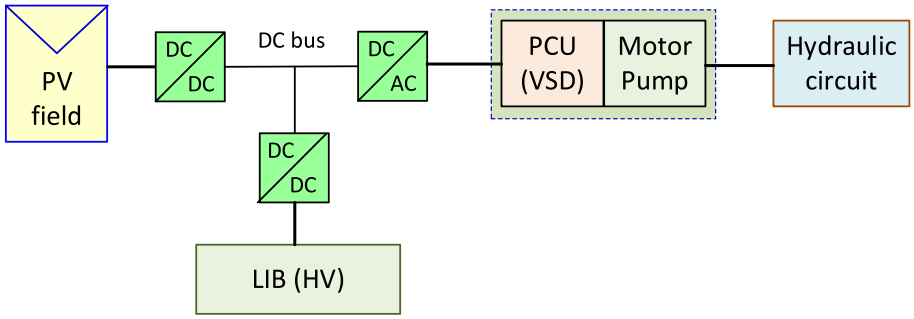

Fig. 2. Block diagram of a battery-based PV pumping system with a DC/DC bidirectional converter.

contributions of this work.

2. High-voltage battery-based water pumping facility: Alternative solutions

The electrical compatibility of the different components that make up a battery-based PV pumping system that uses a three-phase AC drive for the motor-pump group can be solved with two approaches to connecting the battery to the DC-bus of the PV water pumping system: the direct connection (Fig. 1) or by means of a DC/DC bidirectional converter to manage the charging/discharging processes (Fig. 2). The use of a battery controller between the PV array, the battery, and the inverter, as proposed in [9], is less common because of the technical requirements needed for the charge controller and it can be considered a specific case of the use of a DC/DC bidirectional converter.

The direct connection of a battery in a PVWPS was simulated in [52], including a 3.7 kW three-phase motor (with 225 V and 15 A), a 5.48 kW_{pk} PV field, and a battery that used 26 packs of 12 V and 150 Ah (a nominal voltage of 312 V and 46.8 kWh). The battery was connected in parallel with the DC bus of the three-phase VSD, including a switch that controlled the connection of the DC stage (PV field, MPPT power converter, and battery) to the DC-bus of the VSD. The system simulated in [53] used a 360 V and 567 kWh lead-acid battery and the motor-pump group was connected to the output of a PV inverter by means of an on/off motor controller. The direct connection of the 11 kW electrical motor to the AC three-phase system provided by the inverter is not recommended due to surge currents that flow during the switching to on-state (until 326 A vs 29.6 A in steady-state conditions) and the water hammer that could appear during the sudden switching to off-state (without a smooth decrease in motor speed).

There are several recent works including the bidirectional DC/DC converter shown in Fig. 2. The system simulated in [54] used a DC bus voltage of 230 V, a 3.3 kW three-phase motor, a 3.6 kW_{pk} PV field, and a Ni-MH battery with 200 V and 6.5 Ah. Simulated and experimental results were presented in [55] using a DC bus voltage of 400 V, a 2.2 kW three-phase motor, a 2.55 kW_{pk} PV field, and a battery with 200 V and 7 A; while in [56], the system used a DC bus voltage of 600 V, a 3.7 kW three-phase motor, a 4 kW_{pk} PV field, and a battery with 480 V and 42 Ah. The grid-tied solar PVWPS with energy storage presented in [57] also included the DC/DC bidirectional converter to manage battery operation. Grid connection was used either to provide power when the other sources were unavailable, or to feed the energy produced by the PV field back to the grid when the WPS was not in operation and the battery was fully charged. Simulated and experimental results were included using a simulated PV field of 875 W_{pk}, a 160 V and 50 Hz grid, a 750 W switched reluctance motor, and a battery with 240 V and 28 Ah (6.72 kWh).

The use of a bidirectional DC/DC battery power converter is frequent in modern on-grid/off-grid hybrid inverters which include LIBs that can operate in a wide range of battery voltages and capacities, with an AC apparent power in the single-phase models ranging from 3 to 5 kVA [58] and with three-phase models ranging from 5 to 15 kVA (depending on the manufacturer) [59–61]. Because these systems can operate in off-grid mode continuously, most permit the connection of an AC auxiliary generator in the grid-port to keep the system in operation on days with low irradiation levels. All the loads supplied by these hybrid inverters are connected to the AC output port, as proposed in the model simulated in [46].

3. System design and control

In previous studies by the authors of this paper a PVWPS + LIB was first compared with its analogous DPVWPS while maintaining the same PV field configuration and peak power [20]. Subsequently, the energy efficiency of the PVWPS + LIB facility in relation to the selected VSD frequency, was evaluated [21] to determine its optimal operating conditions. Initial experimental results in the PVWPS + LIB facility, described in more detail in [62], were obtained with a low-voltage LIB (48 V) with 3.3 kWh of capacity connected to a 3.7 kW hybrid inverter. Several problems were identified in the operation of the system, as described in [20]. The main issues related to the functioning of the low-voltage LIB hybrid inverter were as follows:

- Improper operation of the MPPT algorithm during the LIB charging intervals, which reduced the PV energy generated and the total pumped water. Increases in daily pumped volume in the range of 8 % to 20 % could be expected with the proper operation of the MPPT algorithm.
- Values provided by the hybrid inverter for P_{PCU_in} and P_{PCU_out}, as defined in [21]. The quantification of some power terms acquired by the hybrid inverter were inaccurate, preventing the direct use of these variables in the management of the system.
- The high stand-by consumption of the hybrid inverter (around 70 W) represented a continuous loss of energy that discharged the battery, with an *SOC* decrease of 25 % during nights, as described in [62].

To overcome these problems, a new hybrid inverter and LIB group was installed in the PVWPS + LIB facility, including the following devices:

- An X1-Hybrid-3.7-D-E grid-connected inverter from SOLAX, with a rated apparent power of 3680 VA in the on-grid output and 4 kVA in the EPS output (emergency power supply) and up to 6 kVA for 10 s in the EPS output [58].
- A high-voltage (HV) lithium-ion battery from SOLAX, model T-BAT SYS-HV (composed by a T-BAT H 5.8 and one battery pack HV11550), with 11.5 kWh of total stored energy (equivalent to 50 Ah), 90 % of maximum *DOD* (10.35 kWh of usable energy), 3.5 kW of maximum power, a maximum charge/discharge current of 35 A, a recommended charge/discharge current of 25 A, and a rated voltage of 230.4 V (the two units were connected in series) [63].

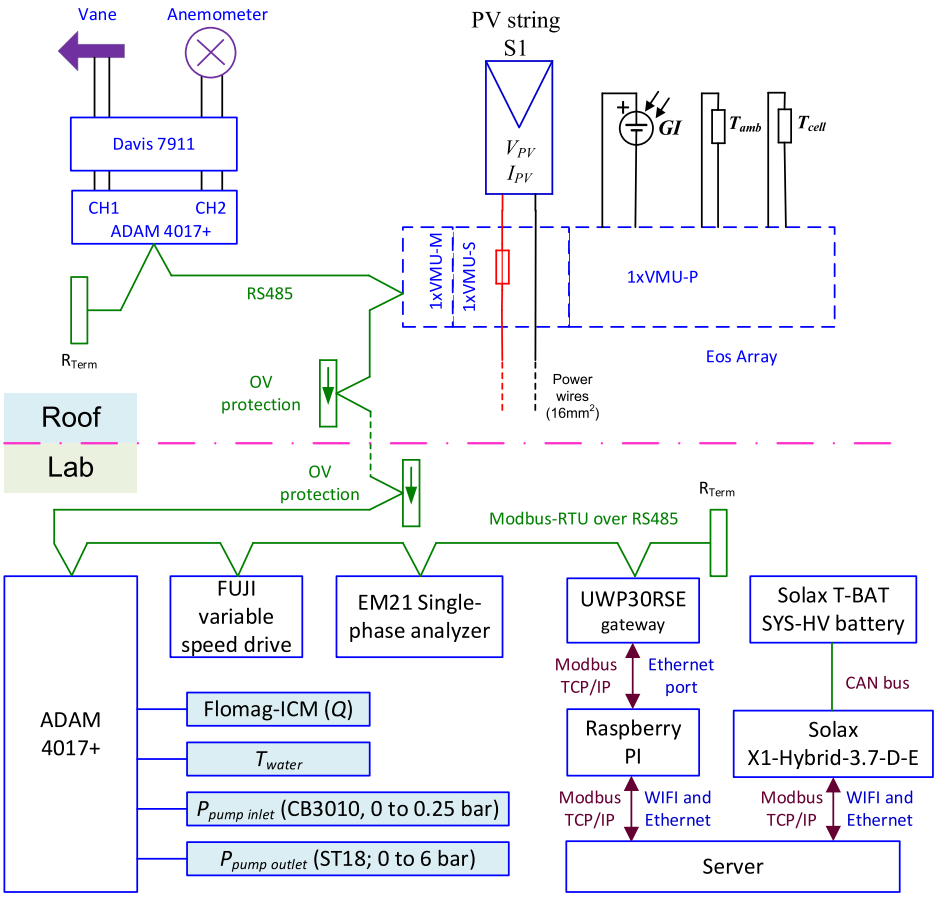

Fig. 3. Block diagram of the devices connected with the RS485 bus in the new version of the PVWPS + LIB facility.

The hybrid inverter was selected considering that the PV field had to be the same as that used in the direct solution and that the AC output had to operate the VSD of the direct solution (approximately 2.2 kW) plus additional loads included in the battery-based solution (energy manager, monitoring systems, etc.). The capacity of the LIB was increased from 3.3 kWh to 12 kWh to operate the water pumping system for longer than one hour and store the average energy that a 2.4 kWpk PV field can produce on an average day in Valencia with 5 PSH.

The monitoring system included in the PVWPS + LIB(HV) facility uses free open-source software tools adapted for this new model of hybrid inverter. The hardware part of the monitoring system is built using the commercial devices described in [62], including an embedded system (Raspberry Pi) and a database (DB) server, as depicted in Fig. 3. Communication between data acquisition nodes is carried out through a wired RS485 protocol. A commercial universal web platform, the UWP 3.0, operates as a communications gateway between all the devices connected through a Modbus-RTU over RS485 and the data acquisition system (using a Modbus with TCP/IP protocol), as shown in Fig. 3 with green lines. The new hybrid inverter uses a CAN bus to communicate with the LIB and an Ethernet connection with the DB server. Data provided by the hybrid inverter have the following resolutions: 0.1 V; 0.1 A; 1 W; 0.1 kWh; 0.01 Hz; 0.1 °C; 1 % for all percentual values (*SOC*; *PF*, etc.).

Several tests of the PVWPS + LIB(HV) facility were carried out following the optimization approach that uses the SBEP of the WPS section, as described in [21]. The greater capacity of the new high-voltage LIB (11.5 kWh vs the 3.3 kWh of the previous low-voltage LIB) combined with the reduced power demand at $f_{VSD} = 37$ Hz (value selected to operate at SEBP) resulted in an extension of the pumping interval (11 h) for a day with 5.29 PSH, as can be seen in Fig. 4, with a connection of the pumping system at the beginning of the day (at 8:13) and disconnecting the WPS at night (19:10). Based on the monitor system described in [62] and modified for this new PVWPS + LIB(HV) facility, values of photovoltaic power (P_{PV}, W) and global irradiance (*GI*, W/m^2) are depicted at the top, while flow rate (*Q*, L/s), total dynamic head (*TDH*, m), and *SOC* (%) are plotted at the bottom of Fig. 4. The total daily volume of water pumped was $V_d = 62.12$ m^3/d, and the daily *SOC* variation was $\Delta SOC_{day} = 1$ % (being $SOC_i = 54$ %, and $SOC_f = 55$ %).

It should be noted that the pumping interval with the PVWPS + LIB facility equipped with low-voltage battery detailed in [62], working at $f_{VSD} = 37$ Hz on a day with PSH = 4.93 (DOY14, 2021), was 8 h:32 min being $V_d = 47.54$ m^3/d. This result is not intended to establish a rigorous comparison since it was not the same installation, nor the same working conditions. However, it can serve to verify the clear advantage of high-voltage LIBs over low-voltage LIBs in installations with these characteristics.

4. Experimental tests

A set of 20 days of operation of the PVWPS + LIB(HV) installation with $f_{VSD} = 37$ Hz was analyzed by processing in Matlab the values provided by the monitoring system, which were recorded every minute ($t_k = 1$ min). Days with differing *GI* profiles were selected to make a comparison across days with differing energy availabilities:

- Sunny days, such as 02/02, 02/03 and 03/13, with $PSH_{02/02} = 5.48$, $PSH_{02/03} = 5.29$, and $PSH_{03/13} = 5.15$.
- Partly cloudy days, such as 02/04, with $PSH_{02/04} = 2.88$.
- Very cloudy days (with rain), such as 02/19, with $PSH_{02/19} = 0.98$.

In addition, a more in-depth daily analysis of the operation of the PVWPS + LIB(HV) facility was made on 03/13.

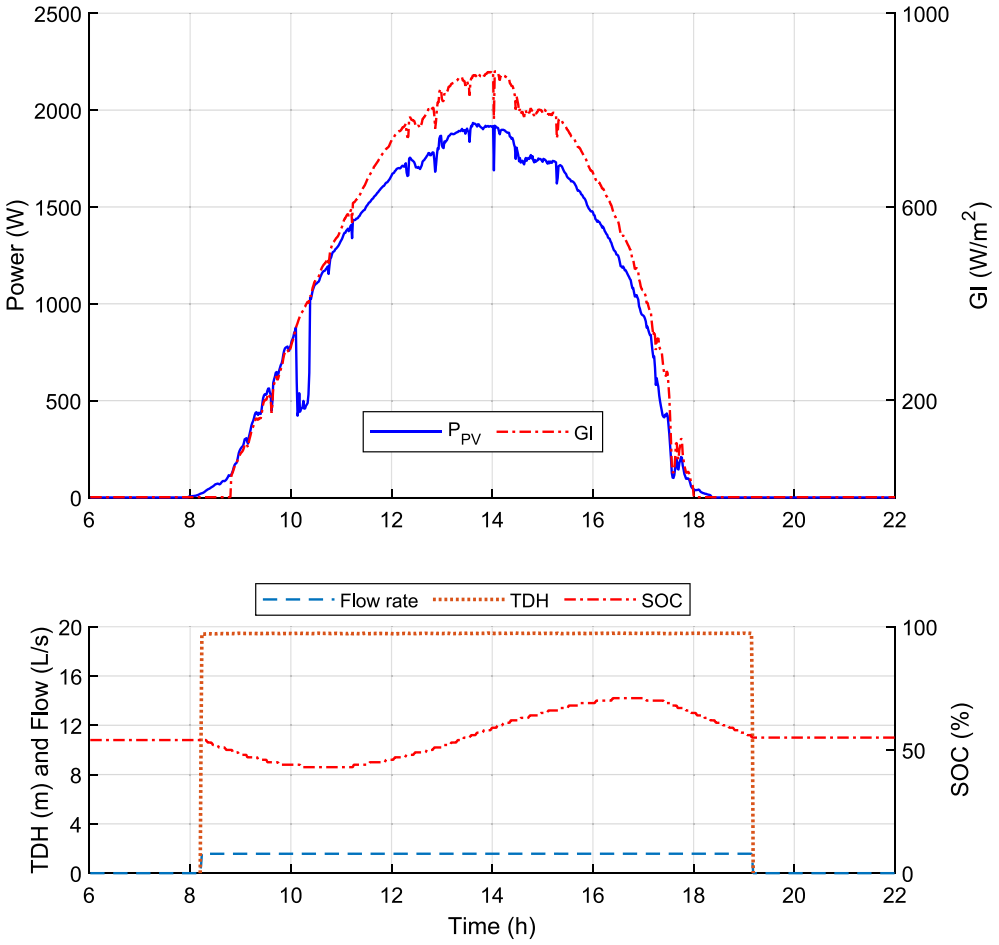

Fig. 4. Main values in the PVWPS + LIB(HV) facility during 02/03 (day of year (DOY) 34, 2022): P_{PV} and *GI* (at the top); *Q*, *TDH*, and *SOC* (at the bottom).

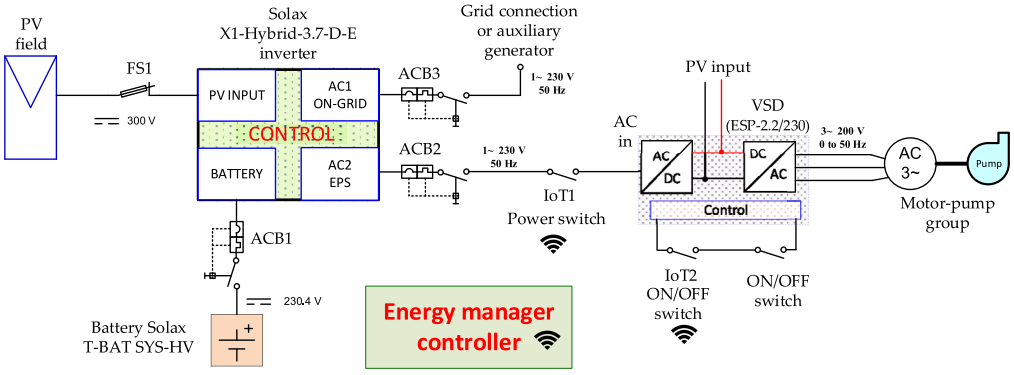

Fig. 5. Block diagram of the PVWPS + LIB(HV) facility.

These experimental tests were also used to verify the usefulness of including an IoT board to manage the WPS operation and study the SBEP of the facility.

4.1. Energy optimization by means of an IoT board

An IoT board to manage the WPS stage was added because of the need to check its correct functioning and to start and stop the WPS at any time of the day and year (even on many occasions at a specific time of day when the facility cannot be accessed). The IoT board selected is an ESP12F_Relay_X2 [64], and its operation can be controlled via the university's Wi-Fi network. The IoT power supply is connected to the EPS port. The two 10 A and 240 V relays included in the IoT board are used to control the WPS operation as follows:

- IoT switch 1 (denoted as IoT1 in Fig. 5): this IoT relay is used to control the operation of a 40 A and 240 V solid-state switch (SSR-40 DA-H [65]). The inclusion of the solid-state switch with a greater rated current than the IoT switch enables reducing the effects of the surge currents that the rectifier in the input of the VSD may require during the charging process of the internal DC bus and so avoiding the large surge currents detailed in [53] (where a VSD was not used).
- IoT switch 2 (denoted as IoT2 in Fig. 5): this IoT relay is connected in series with the ON/OFF switch connected in turn to one of the low-

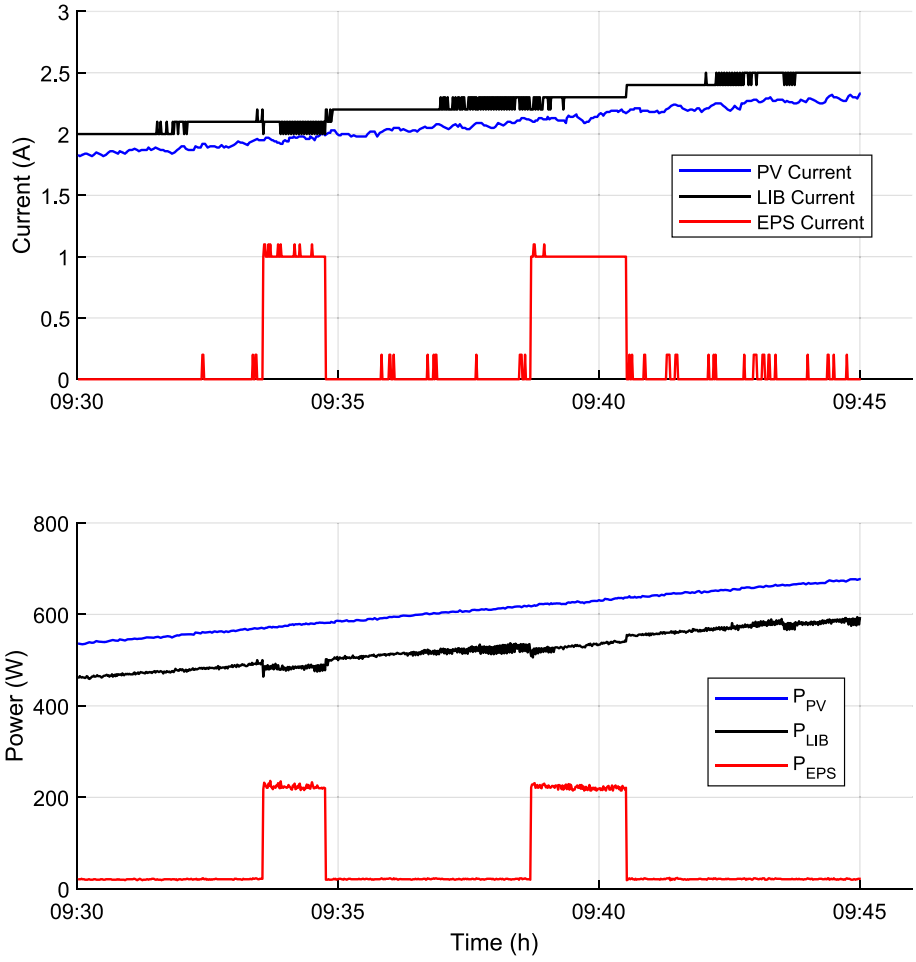

Fig. 6. Currents (at the top) and powers (at the bottom) in the system during the test of the IoT circuit operation on 02/02 (DOY33) from 09:24 to 09:46.

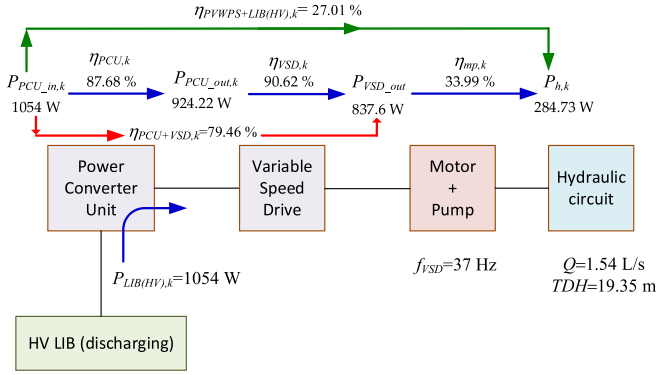

Fig. 7. Main instantaneous values of powers and efficiencies in the PVWPS + LIB(HV) facility obtained from the monitoring system at f_{VSD} = 37 Hz on 03/13 (DOY72).

level control inputs of the VSD. For the remote activation of the WPS, the ON/OFF switch must be ON.

In addition to the capability of activating and deactivating the WPS remotely, the use of the 40 A solid-state switch controlled by the IoT board also reduces current consumption in the EPS output (230 V_{AC} nominal value), changing from 20 mA for the IoT board to 810 mA when the solid-state switch is ON and the VSD is in stand-by mode. The values of these currents were obtained from the hybrid inverter monitoring system and verified using a clamp current meter. The power demand of the IoT board corresponds to less than 5 W, while in the second case (VSD in stand-by mode) it is greater than 185 W, which optimizes the use of the energy stored in the LIB. Values of currents and powers in the hybrid inverter ports (PV, LIB, and EPS) recorded by the monitoring system during a test to verify the energy saving achieved with the IoT board inclusion are shown in Fig. 6. The EPS current when the VSD is in stand-by mode is near to 1 A, while the current demanded by the IoT board is neglectable when the VSD is disconnected. As happened with the previous model of hybrid inverter used in [21] and [62], the values of the EPS power provided by the new hybrid inverter (227 W with the VSD in stand-by mode and 21 W only with the IoT board) correspond more with the apparent power (S, in VA) than to the active power (P, in W) calculated from the measured AC currents.

The reduction in the current consumption produces a reduced discharge of the LIB during the intervals in which the WPS is not operating. The use of the IoT switches is as follows:

- WPS activation: IoT1 is switched on to provide power to the VSD and IoT2 is then activated.
- WPS deactivation: IoT2 is switched off first, and IoT1 is switched off 15 s later. During the delay time between the deactivation of the two switches, the VSD control stage applies a decreasing ramp to the VSD output power and so avoids a water hammer in the hydraulic circuit.

The VSD also enables control actions based on signals from sensors in the WPS, such as high- and low-level sensors in the water tank.

In the following section the main advantages and features of the proposal when compared with the direct PVWPS scheme are detailed.

Table 1
Instantaneous values obtained with the Fluke 435-SII power quality analyzer at f_{VSD} = 37 Hz on 03/13 (DOY72).

P_{PCU_in}	$P_{PCU\_out} = P_{VSD\_in}$	P_{VSD_out}	P_h
1092.19 W	990 W	855.07 W	294.08 W
η_{PCU} = 90.64 %	η_{VSD} = 86.37 %	η_{mp} = 34.39 %	
V_{VSD_out} = 155.06 V	I_{VSD_out} = 4.08 A	Q = 1.55 L/s	TDH = 19.38 m

4.2. Solar best efficiency point for the battery-based water pumping facility

Achieving the highest utilization of the energy produced by the PV field is a challenge in humanitarian emergencies, where useable energy is often scarce. While the operating point of a DPVWPS varies throughout the day (mainly due to the variability of irradiance), in a battery-based scheme it is possible to set a fixed operating point for the water pumping system (VSD and motor-pump group) which should be established at the SBEP. Previous studies in [21], evidence that the SBEP of the WPS facility is found when the frequency of the AC three-phase voltage VSD output is equal to 37 Hz (f_{VSD} = 37 Hz). Although the motor-pump efficiency (η_{mp}) decreases for low values of the f_{VSD}, the VSD efficiency (η_{VSD}) decreases more at the rated frequency (f_{VSD} = 50 Hz). Instantaneous values provided by the monitoring systems for f_{VSD} = 37 Hz are shown in Fig. 7.

The value of the total dynamic head ($TDH_{37\,Hz}$) is calculated in (1) in meters by means of the values obtained from the pressure sensors installed in the pumping outlet (P_{pump_outlet}) and in the bottom of the lab tank (P_{pump_inlet}), including an offset of 0.55 m that considers the relative distances between the sensors and the top and bottom levels of water in the tank.

$$TDH_{37Hz} = P_{pump_{outlet}} - P_{pump_{inlet}} + 0.55 = 19.8 - 1 + 0.55 = 19.35\,\text{m} \quad (1)$$

With the water flow expressed in liters per second (Q = 1.5 L/s), the hydraulic power (P_h) can be calculated in W as follows:

$$P_{h37Hz} = 9.81 \cdot Q_{37Hz} \cdot TDH_{37Hz} = 9.81 \cdot 1.5 \cdot 19.35 = 284.73\,\text{W} \quad (2)$$

The output power in the VSD (P_{VSD_out}) operating at f_{VSD} = 37 Hz is calculated in (3) considering the voltage and current of the VSD three-phase output ($V_{VSD_{out}}$ = 155 V and $I_{VSD_{out}}$ = 4 A) and the power factor of the motor (PF_m = 0.78):

$$P_{VSD\_out\_37Hz} = \sqrt{3} \cdot V_{VSD_{out}} \cdot I_{VSD_{out}} \cdot PF_m = \sqrt{3} \cdot 155 \cdot 4 \cdot 0.78 = 837.6W \quad (3)$$

The value of the input power in the VSD (P_{VSD_in}) referred to as a percentage of its rated value is equal to 42.01 %. Considering that the rated power of the VSD is 2.2 kW, the value P_{VSD_in} is calculated as follows:

$$P_{VSD\_in} = \frac{42.01}{100} \cdot 2.2kW = 924.22W \quad (4)$$

The electrical operating values were verified with a Fluke 435-SII power quality analyzer. The average values for the 10 min of operation with a recording time interval t_k, equal to 5 s are detailed in Table 1, obtaining an average efficiency of the overall system ($\eta_{PVWPS+LIB(HV)}$) equal to 26.92 %. As can be observed, all the values detailed in Fig. 7 and Table 1 are quite similar.

Signals shown in Fig. 8 demonstrate the correct operation of the MPPT algorithm included in the hybrid inverter [58] on sunny and cloudy days, and the loss of energy related to the improper MPPT operation reported in [21] is avoided. During the regular operation of the installation, as in the days shown in Fig. 8, an attempt was made to avoid reaching *SOC* values greater than 80 %, since from that value onwards the power used in the LIB recharge is reduced with respect to the maximum that can be generated by the PV field (concluding in a final nil PV current, as can be seen in some of the graphs included in [66] when *SOC* values of 100 % were reached). The WPS was connected at the beginning of a sunny day (02/03), and the energy was taken from both the PV field and the LIB. After 11:00 (approx.), with *GI* around 450 W/m^2, the *SOC* trend varied and the PV power reached a level (P_{PV} = 1.3 kW) that enabled the WPS operation and the recharge of the LIB (performed until 16:45, when *GI* was below 450 W/m^2). The PVWPS + LIB(HV) facility was pumping with f_{VSD} = 37 Hz from 8:14 to 19:10 (almost 11 h) and maintained the same operating conditions until reaching the same *SOC* as at the end of the previous day's pumping interval (*SOC* = 55 %). A similar approach was used initially for a cloudy day (02/04), and the pump was started at 8:37. However, the low *GI*

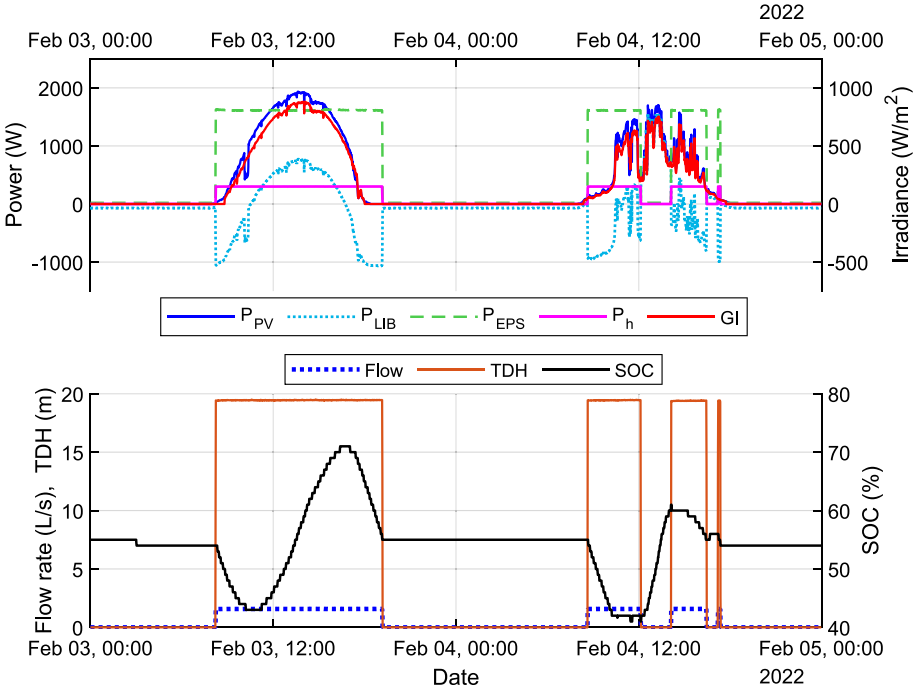

Fig. 8. Main operating values in the facility during 02/03 and 02/04 (DOYs 34 and 35): powers and *GI* (at the top); *Q*, *TDH*, and *SOC* (at the bottom).

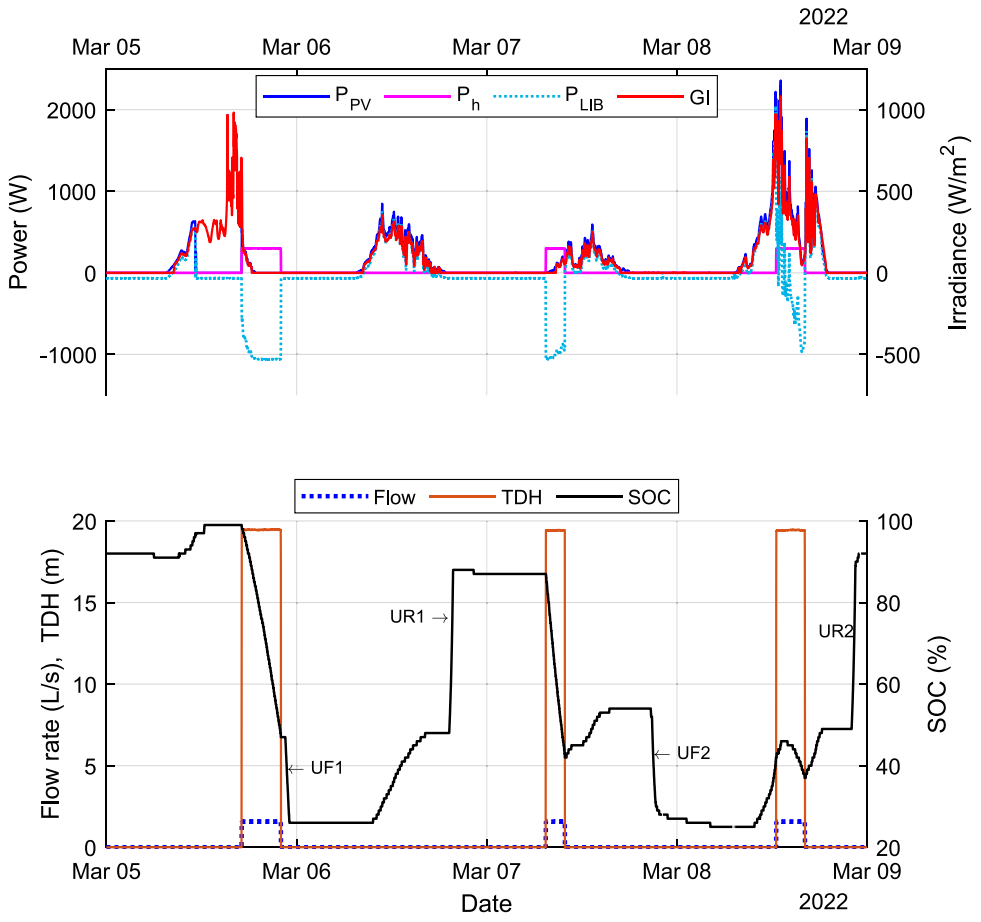

Fig. 9. Main values in the PVWPS + LIB(HV) facility from 03/05 to 03/08 (DOY64 to DOY67, 2022): powers and *GI* (at the top); *Q*, *TDH*, and *SOC* (at the bottom).

profile forced pumping to stop and the final *SOC* was around 55 %. Thus, a total of three pumping intervals can be observed on that day, with a final short interval (10 min) to complete the adjustment of the *SOC* to the desired value. The total pumping interval was about 6 h a day with only 2.88 PSH, and in which direct solar pumping would have worked only during the few intervals when *GI* exceeded $GI_{thre\_start} = 300$ W/m^2 (value of the threshold irradiance in the facility under test, as reported in [20]) and if protection against start/stop cycles (which would have disconnected the system for a long interval to protect the pump) was not activated.

Different aspects to be evaluated, including *SOC*, in battery-based systems in humanitarian aid contexts were described in [45]. As shown in Fig. 8 and commented above, during the tests, an attempt was made to maintain similar levels of *SOC* at the beginning and end of the day to establish daily energy balances in the system, and so the total volume of water pumped in a day (V_d) would correspond to the PV energy generated during the day. The variation of the battery state of charge in one day (ΔSOC_{day}), defined as the difference between final and initial daily *SOC* ($SOC_f - SOC_i$), shows that a significant amount of PV energy was used to charge the battery ($\Delta SOC_{day} > 0$ %) instead of being used to pump water, resulting in a decrease of the V_d value, or that the battery was in discharging mode ($\Delta SOC_{day} < 0$ %) to keep WPS running, which in turn leads to a greater V_d.

4.3. SOC uncontrolled variations

The values of the battery *SOC* provided by the Solax inverter showed, for no apparent reason, sharp increases and decreases when there was no load or power supply connected to the installation, indicating an improper management of the energy available in the LIB. It appeared to be a readjustment of the *SOC* after some internal process of the battery management system (BMS). Several uncontrolled *SOC* variations can be observed in Fig. 9 that show the most important magnitudes during four cloudy days.

The energy generated by the PV field during the first hours of 03/05 (from 7:45 to 11:12) was used to complete the LIB charge and the PV power was nil when the LIB was fully charged (*SOC* = 100 %), in accordance with the behavior observed in some of the graphics included in [66]. The WPS was connected ($Q = 1.55$ L/s at $f_{VSD} = 37$ Hz) from 17:05 to 22:00, with a quite lineal decrease of the *SOC* due to the small PV power generated because of the cloudy weather ($PSH_{03/05} = 2.71$). Shortly after finishing the pumping (at 22:34), the *SOC* dropped from 47 % to 26 % in 33 min with no load connected to the system (denoted as UF1 in Fig. 9), and it remained at 26 % until the sunrise of 03/06 (around 8:00). On this day, only low levels of irradiation were available ($PSH_{03/06} = 1.40$) to charge the LIB, with the *SOC* varying from 26 % (at 9:30) to 48 % (at 18:45, at nightfall). After a short interval without *SOC* variations, an uncontrolled *SOC* rise occurred (UR1), fluctuating from 45 % (at 19:15) to 88 % (at 19:45). Due to the high *SOC* values and the risk of a PV power curtailment, the WPS was connected at 7:27 on 03/07 until *SOC* = 42 % was reached at 9:52. With $PSH_{03/07} = 0.72$, the *SOC* reached 54 % at 18:00 (at sunset). An uncontrolled *SOC* drop (UF2) occurred from 20:40 to 21:30, with *SOC* falling from 54 % to 29 % in around 40 min. In the following 12 h (approx.) the *SOC* showed a smooth variation (LIB self-discharge), until sunrise on 03/08 (around 8:00). A short pumping interval was performed from 12:32 to 16:08, coinciding with peak daytime irradiance. With $PSH_{03/08} = 3.15$, the PVWPS + LIB(HV) pumped water for 3.5 h and the *SOC* varied from 25 % (at 08:00) to 49 % (at 19:00) and remaining constant after the sunset until an uncontrolled *SOC* rise (UR2) from 49 % (at 22:04) to 90 % (at

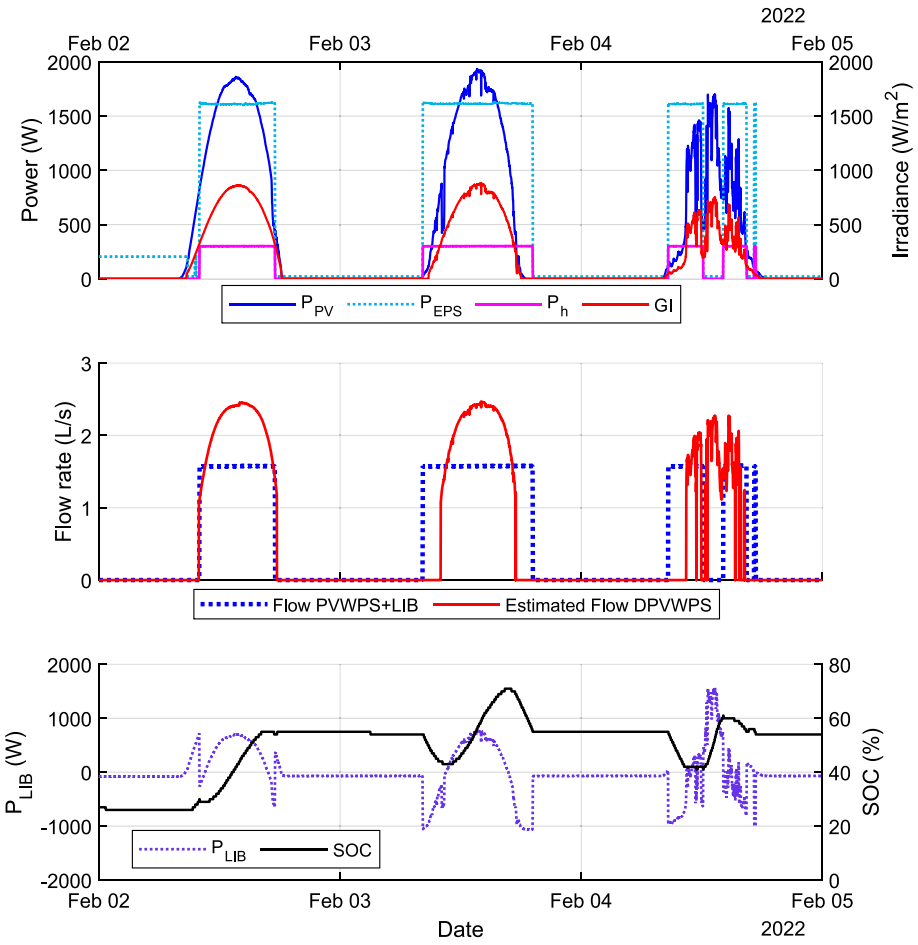

Fig. 10. Main values in the facility from 02/02 to 02/04 (DOYs 33 to 35, 2022): P_{PV}, P_{EPS}, P_h, and *GI* (at the top); *Q* in PVWPS + LIB and estimated *Q* in DPVWPS (at the middle); P_{LIB}, and *SOC* (at the bottom).

23:34).

Although efforts were made to set the same initial and final daily *SOC* values in each experimental test, these uncontrolled *SOC* variations led to the need to apply a compensation for the daily pumped volume based on the *SOC* variation on days with uncontrolled variations or on the daily energy balance in the battery. The test performed in the PVWPS + LIB(HV) facility to obtain the relationship between the daily pumped volume ($\Delta V_{d^*\_LIB\_SOC}$ in m^3/d) and the daily *SOC* variation (ΔSOC_{day}) is described in Appendix A, and resulted in the following expression:

$$\Delta V_{d^*\_LIB\_SOC} = 0.28983 \cdot \Delta SOC_{day} \left(m^3/d\right) \quad (5)$$

As stated in [66], the *SOC* is a primary magnitude of LIBs that is widely used in microgrid control, and is one of the main parameters for the correct management of battery-based pumping systems, together with system alerts and other system variables.

5. Daily analysis of the PVWPS + LIB-HV

Fig. 10 completes the information included in Fig. 8 and shows the relationship between all the powers in the system and the *SOC* for three consecutive days (02/02 to 02/04) with different *GI* profiles and with a correct behavior of the *SOC*. SOC_i on 02/03 and SOC_f on 02/04 were quite similar, and so the compensation due to Δ*SOC* variations for these two days was negligible. The point of operation of the WPS is detailed in Fig. 7. The variation of the *SOC* ($\Delta SOC_{day} = SOC_f - SOC_i$) during the tests on 02/03 and 02/04 was minimal, so no compensation of the pumped volume due to the variation of the *SOC* in the LIB ($\Delta V_{d\_LIB} = f(\Delta SOC)$) was needed in the analysis for these two days (the last pumping interval on 02/04 was used to reach a quite similar *SOC* value to the initial value at the beginning of the test on the preceding day, 02/03). Fig. 10 also includes the estimation of the pumped flow rate with the equivalent DPVWPS solution. To this end, Model 1 of the four models detailed in Appendix B, was used.

An estimation of the V_d pumped by the DPVWPS solution ($V_{d\_DPVWPS\_**}$) using the four fitting models described in Appendix B was carried out for the days analyzed. The estimation of $V_{d\_DPVWPS\_02/03}$ ranged from 53.51 to 57.45 m^3/d, being on average (56.04 ± 1.76) m^3/d (mean ± standard deviation), meanwhile $V_{d\_02/03} = 62.12$ m^3/d (volume pumped with the PVWPS + LIB(HV) facility). Therefore, an increment of the total volume pumped between 8.1 % and 16.1 % (10.85 % on average) was obtained on 02/03 (a sunny day) with the battery-based solution. The total pumping time with the direct solution was estimated at 7:36 (hh:mm), meanwhile the PVWPS + LIB(HV) was pumping during 10:57 in the SBEP. On 02/04, a cloudy day, $V_{d\_DPVWPS\_02/04}$ was on average (29.14 ± 2.76) m^3/d, ranging from 26.23 to 32.31 m^3/d. If these last estimated values are compared with $V_{d\_02/04} = 33.91$ m^3/d, it follows that the battery-based solution pumps between 4.8 % and 29.3 % of extra volume (16.37 % on average) with respect to the DPVWPS. The pumping interval was extended from 5:10, estimated for the DPVWPS, to 6:01 in the battery-based solution. During these two days, with different *GI* profiles, the total volume pumped in the PVWPS + LIB(HV) mode was slightly greater than the values obtained with the estimations made for the DPVWPS mode.

Fig. 11 shows the most relevant magnitudes of the PVWPS + LIB(HV) on 02/19, a very cloudy day with only 0.98 PSH. The *GI* did not reach the threshold irradiance value to start pumping ($GI_{thre\_start} = 301.30$ W/

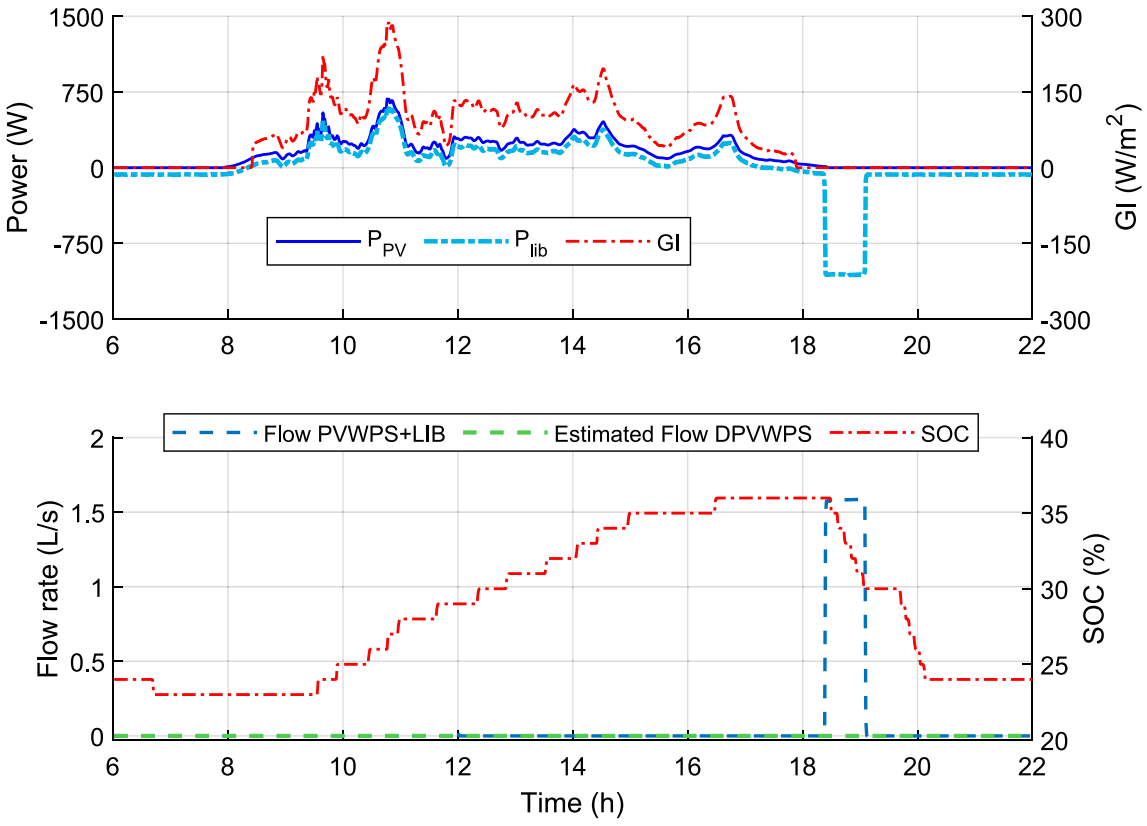

Fig. 11. Values during 02/19 (DOY50): P_{PV}, P_{LIB}, and GI (at the top); Q for PVWPS + LIB(HV), Q estimated for DPVWPS, and SOC (at the bottom).

m^2) so no pumped volume was available in DPVWPS mode during the day, as is shown in this figure (represented as Q estimated for DPVWPS). The battery was charged with the energy produced by the PV field while $GI > 0$ W/m^2, with a SOC variation of between 23 % and 36 %. The pumped volume was $V_{d\_02/19} = 3.99$ m^3/d, obtained during the 44 min that the WPS was connected to reach a final SOC equal to that of sunrise.

A daily analysis of the operation of the PVWPS + LIB(HV) facility was performed on 03/13. This day was selected because the variation of the SOC during the day was minimal ($\Delta SOC_{day} = +1$ %, with $SOC_i = 53$ % and $SOC_f = 54$ %), and so only a very small correction of the pumped volume was required considering (5):

$$\Delta V_{d^*\_LIB\_SOC\_DOY72} = 0.28983 \cdot \Delta SOC_{day} = 0.28983 \cdot 1\% \approx 0.29\, m^3 \quad (6)$$

As can be seen in the P_{PV} profile shown in Fig. 12, the presence of clouds during the day produced rapid variations in PV power, with GI sometimes (as at 11:15) reaching levels smaller than 200 W/m^2 – a value that corresponds to the GI_{thre_stop} in the DPVWPS mode. The WPS was operating continuously with $f_{VSD} = 37$ Hz for 10.77 h (from 8:04 to 18:50). The charging of the LIB took place for $P_{PV} > 1.1$ kW (approx.) from 10:00 to 16:30 (approx.) as is shown by the increase in SOC during this interval.

The approximate operating conditions of the system on 03/13 are detailed in Fig. 7 and Table 1 (see Section 4.2), and some small variation in the average values (shown below) can be explained by the differing WPS operating conditions (e.g., ambient and water temperatures). The average values of the main variables while pumping ($Q > 0$ L/s) are detailed in Table 2, and $\eta_{PVWPS+LIB\_AV} = 27.23$ % (as the product of the three values provided in the third row).

The total volume pumped in a day (V_d) can be calculated summing the pumped volume in each acquisition interval ($V_{d,k}$) obtained using the values of Q recorded by the monitoring system (Q_k) multiplied by the acquisition interval (t_k):

$$V_{d,k} = Q_k \cdot t_k \rightarrow V_d = \sum\nolimits_k V_{d,k} = t_k \sum\nolimits_k Q_k \quad (7)$$

An approximate value of the total volume pumped on this day is $V_{d\_03/13} \approx 61.23$ m^3, as obtained using the average Q (Q_{AV}) and the pumping time (t_{pump}):

$$V_{d\_DOY72} = Q_{AV} \cdot t_{pump} = 1.58 \frac{L}{s} \cdot \frac{3600 s}{1 h} \cdot \frac{1 m^3}{1000 L} \cdot 10.77 h \approx 61.23 m^3 \quad (8)$$

If the value calculated in (6) is added, the total volume pumped on this day (including the SOC correction) could reach 61.52 m^3. Fig. 13 shows the variations of GI and P_{PV} together with the values of Q obtained with the PVWPS + LIB(HV) facility on 03/13, as well as Q estimated in the DPVWPS for the same day using the second estimation approach presented in Appendix B (equation B(2). When applying the four approaches for the estimation of $V_{d\_DPVWPS\_03/13}$, the obtained values ranged between 51.87 and 57.24 m^3/d, with the average being (55.10 ± 2.43) m^3/d, which resulted in an average increase in the total pumped volume in the battery-based solution of between 6.9 % and 18 %, 11.1 % (considering $V_{d\_03/13} = 61.23$ m^3/d).

The above estimations were made assuming that the hybrid inverter performed the SOC calculation correctly. Although the variation of the SOC throughout 03/13 was positive ($\Delta SOC_{03/13} = 1$ %, with $SOC_i = 53$ % and $SOC_f = 54$ %) and represented an increase in the energy stored in the LIB, the results obtained using the battery power (P_{LIB}) disagree with the above values and produce the following results:

- Energy charged in the LIB: +2.45 kWh.
- Energy discharged from the LIB: −3.61 kWh.
- Energy balance (EB) in the LIB: $\Delta E_{LIB\_03/13} =$ − 1.17 kWh

This result of − 1.17 kWh shows that the LIB discharge was greater than the charge, and this should correspond to a negative variation of

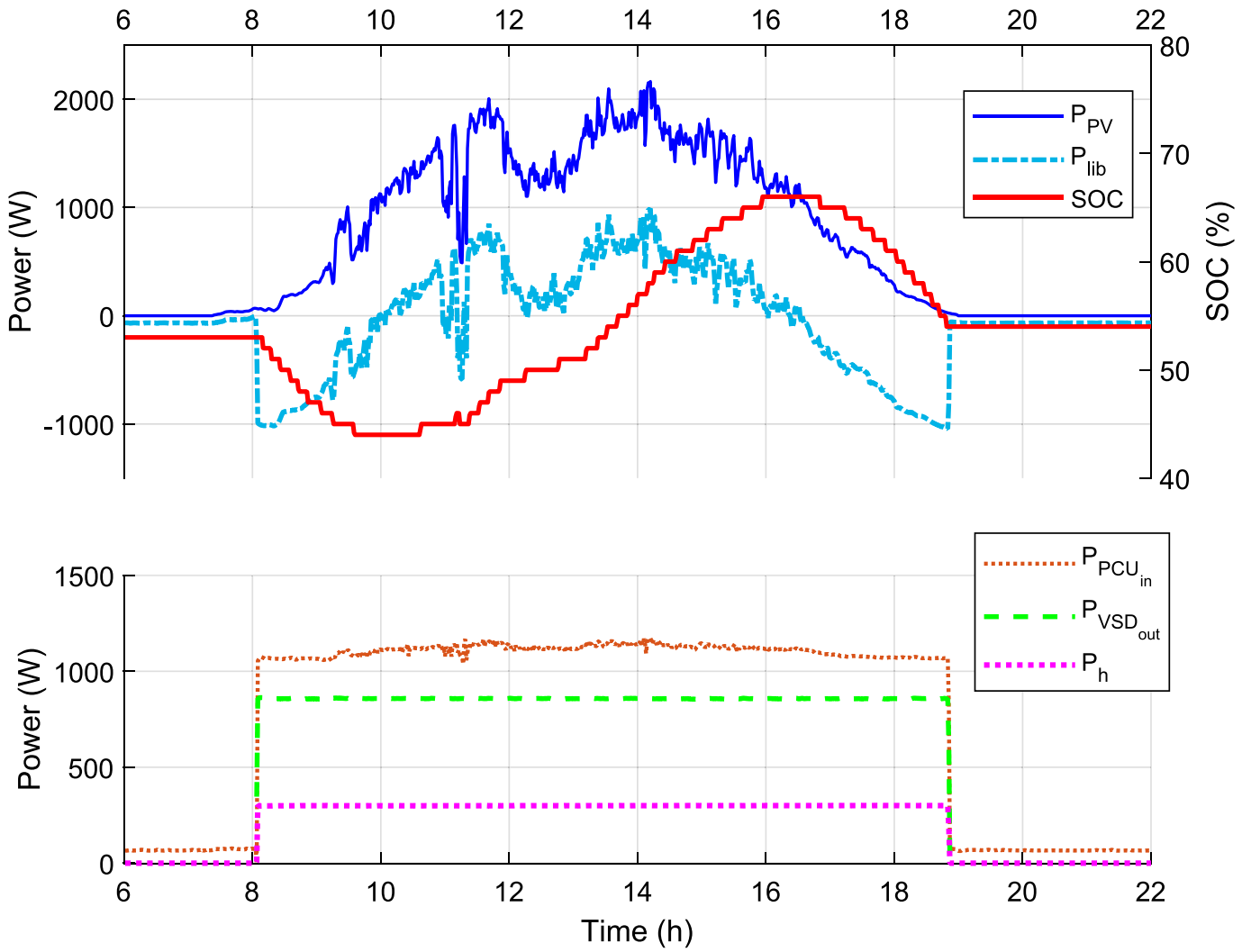

Fig. 12. Values of P_{PV}, P_{LIB}, and SOC (at the top), and P_{PCU_in}, P_{VSD_out} and P_h (at the bottom) in the PVWPS + LIB(HV) facility during 03/13 (DOY72).

Table 2
Average values in the PVWPS + LIB(HV) system during pumping on 03/13 (DOY72).

$P_{PCU\_in\_AV}$	$P_{PCU\_out\_AV} = P_{VSD\_in\_AV}$	$P_{VSD\_out\_AV}$	P_{h_AV}
1099.93 W	928.26 W	857.7 W	299.64 W
$\eta_{PCU\_AV} = 84.39$ %	$\eta_{VSD\_AV} = 92.39$ %	$\eta_{mp\_AV} = 34.93$ %	
$V_{VSD\_out} = 155.04$ V	$I_{VSD\_out} = 4.09$ A	$Q = 1.58$ L/s	$TDH = 19.4\ m$

the SOC in the range of − 10 %:

$$\Delta SOC_{(EB)DOY72} = \frac{-1.17kWh}{11.5kWh}100 \approx -10.2\% \quad (9)$$

This outcome disagrees with the value $\Delta SOC_{03/13} = 1$ % provided by the hybrid inverter. The manufacturer of the LIB and hybrid inverter is working on a solution for this problem. This is not an isolated case and occurs systematically – affecting calculations of the daily V_d and so preventing a correct control of the system operation. Fig. 14 includes all the energies and performance ratios (PR) in the PVWPS + LIB(HV) facility during the test carried out on 03/13. Although most of the values appearing in Fig. 14 were directly provided by the monitoring system, the power in the input of the VSD (P_{VSD_in}) while the WPS was in operation ($Q > 0$ L/s) was corrected using the value obtained with the Fluke power analyzer (928.67 W, as detailed in Table 2).

The variation of pumped volume related to the total energy LIB balance (−1.17 kWh), denoted as $V_{d^*\_LIB\_Bal1}$, is calculated as follows:

$$\Delta V_{d^*\_LIB\_Bal1\_DOY72} = Q_{AV}\cdot\frac{\Delta E_{LIB}}{P_{PCU_{in}}} = 1.58\frac{L}{s}\frac{3600s}{1h}\frac{1m^3}{1000L}\frac{-1.17kWh}{1.09kW} = -6.1m^3 \quad (10)$$

This value corresponds to a 10 % of reduction considering $V_{d\_03/13} = 61.23$ m^3/d. The energy discharged from the LIB while the WPS was not in operation ($Q = 0$ L/s between 0:00 to 08:03 and from 18:52 to 23:59) was equal to −0.85 kWh (obtained by summing all the values provided by the hybrid inverter). The value of −0.85 kWh corresponds to an approximate demand of 65 W during the 13.16 h in which the system was not pumping. This energy could be saved by:

- Reducing the stand-by consumption of the hybrid inverter operating in the EPS mode (a problem that can only be addressed by the inverter manufacturer).
- Disconnecting the LIB battery from the hybrid inverter (by adding a manual or automatic circuit breaker).

This energy savings of 0.85 kWh can be converted into pumped volume estimates with the values shown in Table 2:

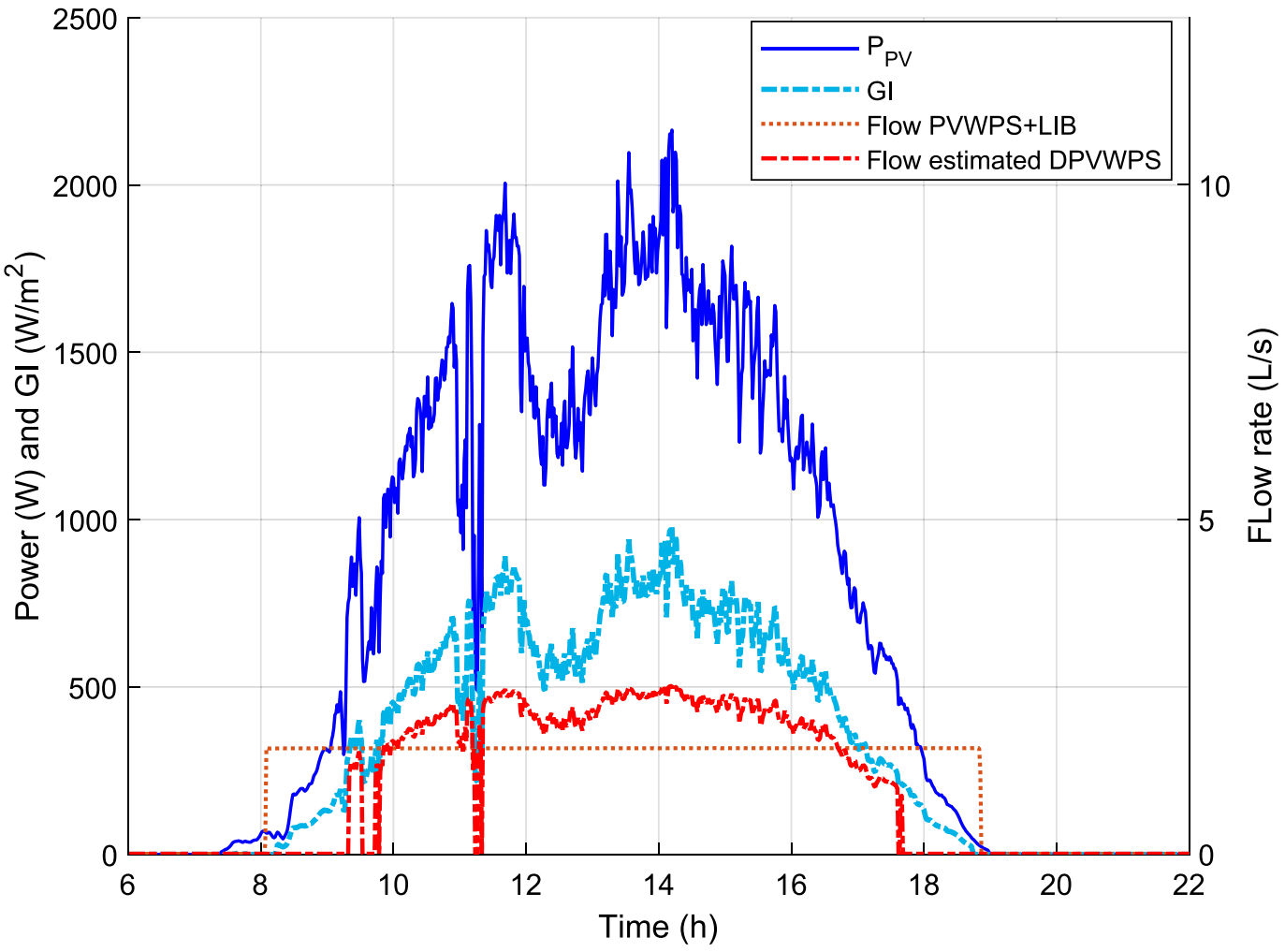

Fig. 13. Values on 03/13 (DOY72): P_{PV}, *GI*, *Q* for PVWPS + LIB(HV), and *Q* estimated for the DPVWPS mode calculated with Estimation 2 of Appendix B.

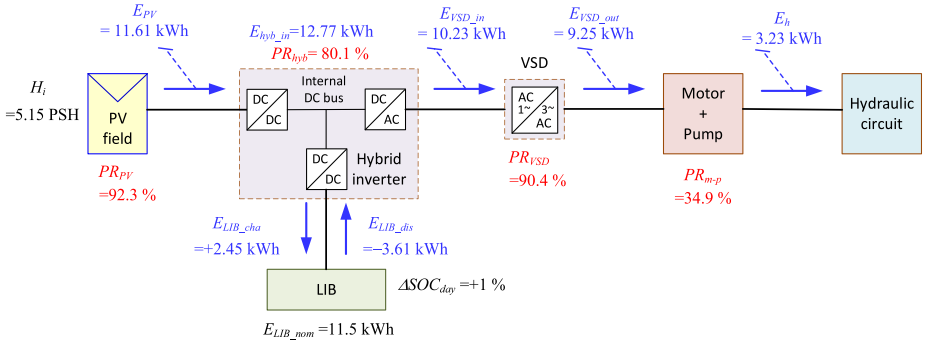

Fig. 14. Block diagram of a PVWPS + LIB facility including energies and performance ratios in the system during 03/13 (DOY72).

$$\Delta V_{d^*\_LIB\_stand-by\_DOY72} = Q_{AV}\cdot t_{stand-by} = Q_{AV}\cdot\frac{E_{LIBstand-by}}{P_{PCU_{in}}}$$
$$= 1.58\frac{L}{s}\cdot\frac{3600s}{1h}\cdot\frac{1m^3}{1000L}\cdot\frac{0.85kWh}{1.09kW} = 4.43m^3 \quad (11)$$

This value is a 7.2 % increase on $V_{d\_03/13}$. The difference between the energy balance in the LIB (- 1.17 kWh) and the energy consumption in the stand-by mode (-0.85 kWh) can be seen as if some of the LIB energy were converted into additional volume pumped during this day. The variation of pumped volume related to this energy balance (denoted as $\Delta V_{d^*\_LIB\_Bal2}$) is calculated as follows:

$$\Delta V_{d^*\_LIB\_Bal2\_DOY72} = Q_{AV}\cdot\frac{E_{LIB_{balance}}}{P_{PCU_{in}}}$$
$$= 1.58\frac{L}{s}\cdot\frac{3600s}{1h}\cdot\frac{1m^3}{1000L}\cdot\frac{(+1.17-0.85)kWh}{1.09kW} = 1.67m^3 \quad (12)$$

This value is a 2.7 % reduction on $V_{d\_03/13}$. As a summary of the study performed on 03/13 and considering that the hybrid inverter correctly performed the *SOC* management, the operation of the PVWPS + LIB(HV) presents the following advantages:

Table 3
Summary of the results obtained on different days and average values (AV) and standard error (SD) considering a set of 20 days in PVWPS + LIB(HV) mode.

Month/day	02/02	02/03	02/04	02/19	03/13	$(AV)_{20\ days}$	$(SD)_{20\ days}$
PSH (kWh/m^2)	5.48	5.29	2.88	0.98	5.15	4.20	1.90
TDH_{AV} (m)	19.42	19.43	19.31	18.53	19.34	19.29	0.23
V_d (m^3/d)	42.65	62.12	33.91	3.99	61.23	41.09	19.61
$V_{d^*\_LIB\_SOC}$ (m^3/d)	42.69	62.12	33.91	3.99	61.23	42.74	19.95
$V_{d^*\_LIB\_Bal1}$ (m^3/d)	54.11	55.33	27.23	3.15	55.32	42.19	22.31
$V_{d^*\_LIB\_Bal2}$ (m^3/d)	59.56	59.97	32.49	7.94	59.65	46.49	21.94
E_h (kWh/d)	2.26	3.29	1.79	0.21	3.23	2.17	1.03
E_{PV} (kWh/d)	12.06	11.76	6.58	2.24	11.67	9.39	4.15
ΔE_{LIB} (kWh/d)	2.29	−1.33	−1.28	−0.16	−1.15	0.24	1.81
E_{LIB_cha} (kWh/d)	3.65	3.04	2.39	1.48	2.45	3.26	1.18
E_{LIB_dis} (kWh/d)	−1.37	−4.37	−3.67	−1.64	−3.60	−3.01	1.23
E_{LIB_dis2} (kWh/d)	−1.09	−0.91	−1.01	−0.89	−0.84	−0.83	0.17
SOC_i (%)	0.26	0.54	0.55	0.23	0.53	0.42	0.18
SOC_f (%)	0.55	0.55	0.54	0.24	0.54	0.52	0.14
E_{VSD_in} (kWh/d)	15.47	10.47	6.01	1.07	10.25	8.53	4.93
E_{PCU_in} (kWh/d)	9.77	13.09	7.86	2.40	12.82	9.12	3.56
E_{VSD_out} (kWh/d)	6.45	9.39	5.12	0.60	9.25	6.16	2.92
PR_{PV} (%)	90.17	91.18	93.70	94.34	92.86	91.68	89.29
$PR_{PCU+VSD}$ (%)	65.95	71.76	65.14	25.03	72.18	63.93	11.51
PR_{mp} (%)	35.03	35.03	34.98	34.92	34.91	35.08	0.36
$PR_{PVWPS+LIB}$ (%)	18.72	27.98	27.23	9.35	27.68	23.61	6.92
$PR_{overall}$ (%)	2.65	4.01	4.01	1.39	4.04	3.45	1.06
$\eta_{PCU+VSD\_AV}$ (%)	75.82	77.16	78.47	79.39	77.46	77.70	1.51
η_{mp_AV} (%)	35.01	35.02	34.87	34.37	34.88	35.02	0.40
η_{PV_AV} (%)	14.19	14.35	14.66	14.51	14.56	14.49	0.34
η_{PV_AV} (%) if Q > 0	14.16	14.35	14.70	14.55	14.56	14.37	0.38
$\eta_{*PVWPS*\_AV}$ (%)	26.55	27.03	27.40	27.04	27.05	27.23	0.57
t_{pump} (min)	452	658	361	44	648	427	198
f_{VSD_AV} (Hz)	36.96	36.96	36.70	36.96	36.97	36.90	0.10

Table 4
Estimation of the pumped volume obtained with the DPVWPS under different conditions.

Month/day	02/02	02/03	02/04	02/19	03/13	$(AV)_{20\ days}$	$(SD)_{20\ days}$
$V_{d\_DPVWPS\_est1}$ (m^3/d)	58.98	56.95	30.47	0.00	56.67	41.37	17.70
$V_{d\_DPVWPS\_est2}$ (m^3/d)	59.46	57.45	32.31	0.00	57.24	42.71	21.66
$V_{d\_DPVWPS\_est3}$ (m^3/d)	55.29	53.51	26.23	0.00	51.87	38.03	17.97
$V_{d\_DPVWPS\_est4}$ (m^3/d)	58.58	56.26	27.55	4.86	54.63	43.26	22.71
$(mean \pm SD)_{4\ models}$	58.08 ± 1.89	56.04 ± 1.76	29.14 ± 2.76	–	55.10 ± 2.43		

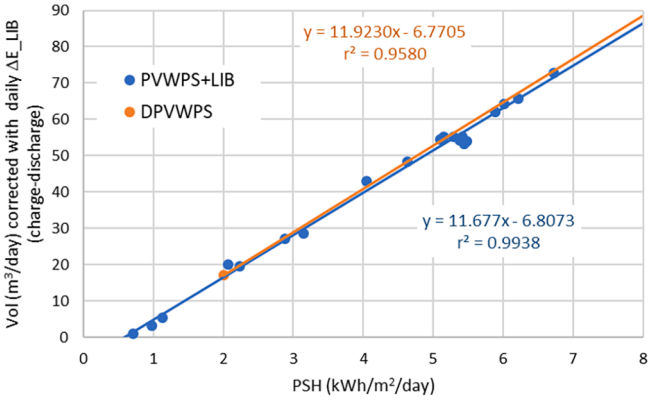

Fig. 15. Comparison between the daily pumped volume obtained with PVWPS + LIB(HV) including the LIB energy balance correction and the volume calculated for the DPVWPS with Estimation 4.

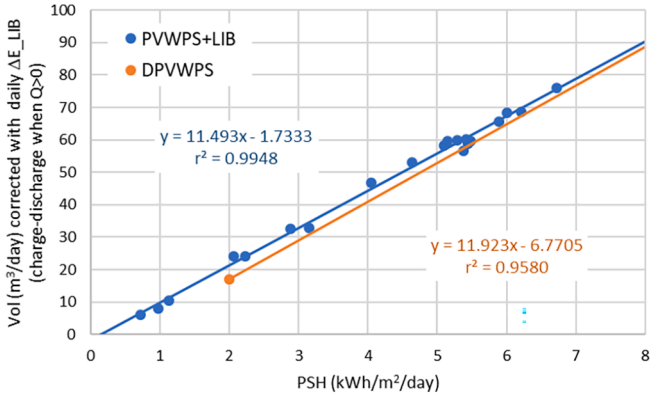

Fig. 16. Comparison between the daily pumped volume obtained with PVWPS + LIB(HV) and the calculated volume for the DPVWPS with Estimation 4, including the LIB energy balance correction and avoiding losses in the PCU when there is no pumping.

- A pumped volume of between 5.5 % and 12 % is greater than that obtained with the corresponding DPVWPS scheme.
- An extended pumping time is achieved with the battery-based solution (10.77 h with a fixed Q) versus the direct solution (around 8 h of pumping with a variable Q).

If the SOC values provided by the hybrid inverter are inaccurate (as it seems) and the pumped volume is corrected from the energy balance in the battery, then the pumped volume with the PVWPS + LIB(HV) is slightly lower than that obtained with the DPVWPS.

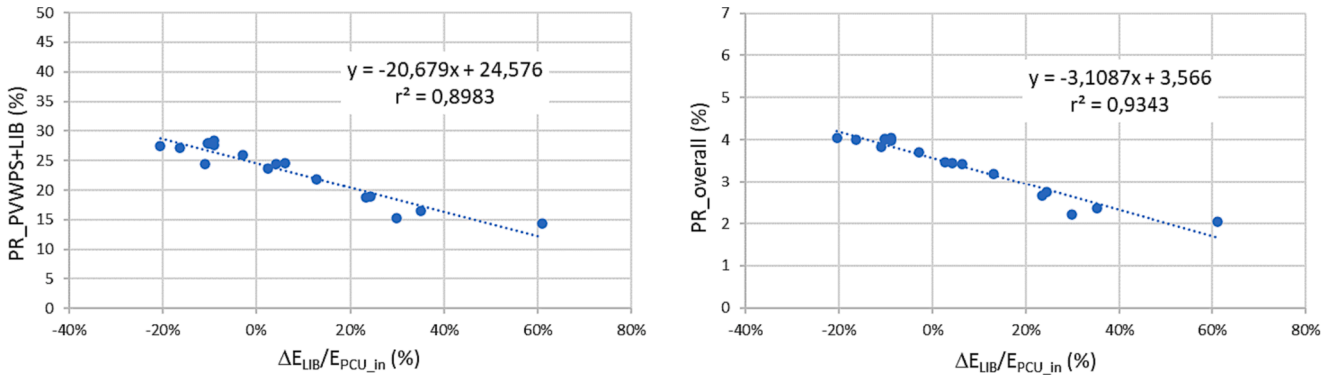

Fig. 17. Relationship between the percentual values of the ratio $\Delta E_{LIB}/E_{PCU\_in}$ with $PR_{PVWPS+LIB}$ (on the left) and $PR_{overall}$ (on the right) on days with irradiation greater than 2 PSH.

Table 5
PR variation after the correction of the volume and the compensation of the energy balance in the LIB.

Month/day	02/02	02/03	02/04	02/19	03/13	Average	Standard deviation (SD)
ΔE_{LIB} (kWh/d)	+2.29	−1.33	−1.28	−0.16	−1.15	+0.24	1.81
$PR_{PVWPS+LIB}$ (%)	18.72	27.98	27.23	9.35	27.68	23.61	6.92
↓	↓	↓	↓	↓	↓	↓	↓
$PR_{PVWPS+LIB*}$ (%)	23.76	24.92	21.86	7.39	25.00	24.25	6.45
$PR_{overall}$ (%)	2.65	4.01	4.01	1.39	4.04	3.45	1.06
↓	↓	↓	↓	↓	↓	↓	↓
$PR_{overall*}$ (%)	3.37	3.57	3.22	1.10	3.65	3.54	0.91

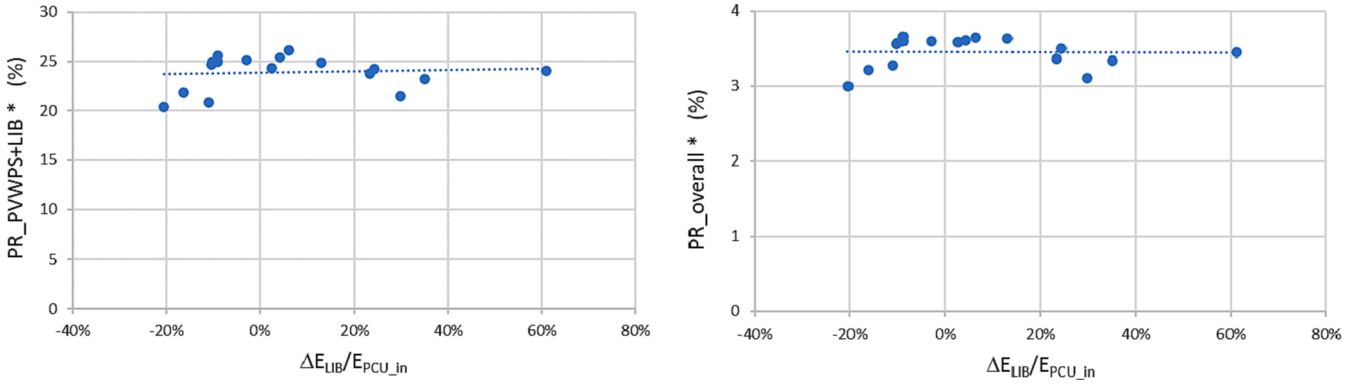

Fig. 18. Relationship between the ratio $\Delta E_{LIB}/E_{PCU\_in}$ and $PR_{PVWPS+LIB*}$ (on the left) and $PR_{overall*}$ (on the right) in days with irradiation greater than 2 PSH.

6. Discussion

Table 3 presents a summary of the main values calculated for the PVWPS + LIB(HV) facility operating under a constant f_{VSD} = 37 Hz. As discussed for 03/13, the term $V_{d*\_LIB\_Bal1}$ is the total pumped volume corrected with the total variation of LIB energy throughout the day ($\Delta E_{LIB} = E_{LIB\_cha} + E_{LIB\_dis}$) and $V_{d*\_LIB\_Bal2}$ includes the surplus volume obtained if the stand-by losses of the hybrid inverter while the WPS is not pumping are ignored. Average values are calculated considering 20 days of operation for the battery-based solution.

As a comparison between low- and high-voltage battery-based WPS, the average values for 15 days of operation described in [20], with f_{VSD} = 50 Hz, PSH_{AV} = 5.26, produced a pumping time of 3 h:35 min and V_{d_AV} = 33.39 m^3/d; while the results with the HV battery (average values for 20 days), with f_{VSD} = 37 Hz, PSH_{AV} = 4.20, produced a pumping time of 4 h:07 min and V_{d_AV} = 41.09 m^3/d. As can be verified, the solution with the hybrid inverter using the high voltage battery almost doubles the pumping time and increases the pumped volume by 23 % – despite a 20 % lower average PSH.

Using the approaches described in Appendix B, the estimated pumped volumes obtained with the equivalent DPVWPS are shown in Table 4 for the same specific days together with the average values for the 20 days of the study.

The corrected pumped volumes considering the *SOC* show notable daily differences with respect to the estimated volumes in DPVWPS mode. This does not happen when the pumped volumes are corrected using the energy balance approach. Therefore, the *SOC*-corrected volume will not be used for comparisons.

Comparison of the volume pumped by the PVWPS + LIB(HV) on sunny days (03/13, 02/02, and 02/03) with the estimation for the DPVWPS that seems to provide the greatest approximation to real V_d ($V_{d\_DPVWPS\_est2}$) shows that in all cases the volume pumped with DPVWPS is between $V_{d*\_LIB\_Bal1}$ (considering the total energy balance in the LIB) and $V_{d*\_LIB\_Bal2}$ (this estimation neglects the battery discharge produced by the stand-by losses in the hybrid inverter).

The main advantage of the battery system is evident on days with very low insolation, such as 02/19. On cloudy and rainy days, such as 02/19, there would be no water pumping in DPVWPS mode. However, by using the PV energy stored throughout the day in the LIB it is possible to pump up to 3.15 m^3/d, which could be increased to 7.84 m^3/d if the

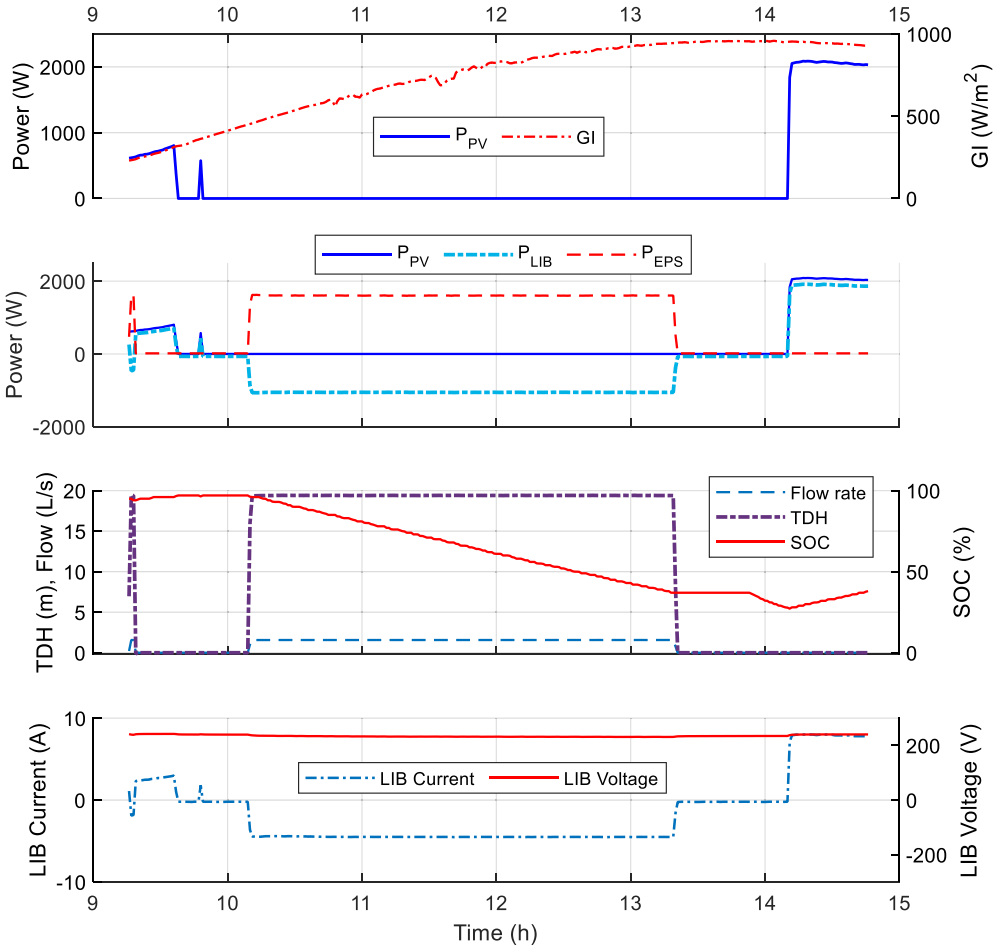

Fig. A1. Values acquired in the WPS from 09:15 to 14:45 on 03/09 (DOY68) during the battery discharge test with f_{VSD} = 37 Hz and the PV array disconnected. *GI* and P_{PV}; P_{PV}, P_{EPS} and P_{LIB}; *Q*, *TDH*, and *SOC*; I_{LIB} and V_{LIB}; (from top to bottom).

Table A1
Values obtained in the LIB discharging test and test conditions.

	SOC (%)	V_{LIB} (V)	I_{LIB} (A)	P_{LIB} (W)	P_{EPS} (W)
Initial values (at 10:10)	96	238	−4.45	−1054	924
Final values (at 13:20):	37	231	−4.5	−1054	924
P_{Grid}= P_{PV} = 0 W	Q = 1.5 L/s (constant during all the interval)				
Inlet pressure: 1 m	Outlet pressure: 19.85 m				
P_{VSD_in} = 42.01 %	f_{VSD} = 37 Hz	V_{VSD_out} = 155 V	I_{VSD_out} = 4 A		

SOLAX control reduced the standby losses when there is no pumping (no energy consumption at the output).

The average water volume pumped in the 20 days of operation with the PVWPS + LIB(HV) system related to the total energy balance ($V_{d^*\_LIB\_Bal1}$ = 42.19 m^3/d in Table 3), is slightly smaller than the best estimation for the DPVWPS model (42.71 m^3/d in Table 4 with Estimation 2, which considers only sunny days), although this is 9.86 % more than that obtained with Estimation 3 (38.03 m^3/d, considering days with variable radiation). If the SOLAX standby losses could be avoided when there is no electrical load connected to the EPS-output (i.e., considering only E_{LIB_dis2}), the water pumped in the 20 days of operation with the PVWPS + LIB(HV) system could be increased by 10.2 % (from 42.19 m^3/d to 46.49 m^3/d, detailed as $V_{d^*\_LIB\_Bal2}$ in Table 3).

The pumped volume obtained with the PVWPS + LIB(HV), corrected with the volume due to the energy balance in the LIB, is compared in Fig. 15 with the volume calculated for the DPVWPS for the same days under Estimation 4. Both trend lines are quite similar except for very cloudy days, although the estimated volume pumped in DPVWPS was always slightly higher (on days with the highest and lowest PSH values). The conditions applied in the fitting analysis do not correctly match with what was observed on 02/19, when the PVWPS + LIB(HV) pumped a small volume of water while DPVWPS would have pumped no water due to the low *GI* levels during the day. As can be seen in Fig. 15, the trend line of the DPWPS starts at 2 PSH, and at lower values, there will be no pumping or the pumped volume will be very small (since the minimum irradiance threshold value for the start of pumping is not reached and start/stop cycles on cloudy days are limited). It should also be mentioned that in different experimental tests (prior to those included in this paper) with the installation working in direct mode, it was verified that 60 % of the days in which the PSH value was less than 2 there was no, or minimal, water pumped.

Fig. 16 shows the comparison between the pumped volume obtained with the PVWPS + LIB(HV) when corrected by including the energy balance in the LIB and considering only the losses in the hybrid inverter when $Q > 0$ L/s (E_{LIB_dis2} instead of E_{LIB_dis}). As can be observed by comparing both lines, the PVWPS + LIB(HV) mode pumps more volume for all the days, and this difference is slightly more appreciable on days with low PSH values (corroborating the analysis made for 02/19). It should also be noted that the intercept (independent term), which in the linear adjustments represented in Fig. 15 and Fig. 16 is negative, and this shows that the unavoidable and therefore minimal losses in the system are lower when discarding the losses in the PCU when no water is

pumped (Fig. 16).

The following figures show, for the days with irradiation greater than 2 PSH, the relationship between $PR_{PVWPS+LIB}$ (Fig. 17-left) and $PR_{overall}$ (Fig. 17-right) with respect to the ratio $\frac{\Delta E_{LIB}}{E_{PCU\_in}}$. The fitting analysis yields $PR_{PVWPS+LIB} = 24.576$ % and $PR_{overall} = 3.566$ % on days with $\Delta E_{LIB} = 0$. These values are greater than those provided in Table 3 (average of 23.61 % and 3.45 %, respectively in the 20 days of study), where the days with irradiation below 2 PSH are also included.

The battery contributes decisively to pumping on cloudy days with low and variable *GI* and provides the energy necessary to avoid stops due to the passage of clouds [42], although the cost is low system efficiency. This is observed on 02/19 (Table 3) when the system pumped at least 3.15 m^3/d in PVWPS + LIB mode, while it would have pumped nothing in DPWPS mode, showing values of $PR_{PVWPS+LIB}$ and $PR_{overall}$ of 9.35 % and 1.39 % respectively, much lower than the average values for all days.

Just as the pumped volume is corrected to facilitate comparison between days, it seems reasonable that the factors affected by the higher or lower consumption of energy stored in the battery should also be corrected, specifically $PR_{PVWPS+LIB}$ and $PR_{overall}$. Hydraulic energy (E_h) can be calculated as follows:

$$V_d = \frac{E_h}{\rho \cdot g \cdot TDH_{AV}} \rightarrow E_h = \rho \cdot g \cdot TDH_{AV} \cdot V_d \tag{13}$$

where ρ *is* the water density (1000 kg/m^3) and g is the acceleration of gravity (9.81 m/s^2). The corrected hydraulic energy (E_{h*}) is obtained as follows:

$$E_{h*} = \rho \cdot g \cdot TDH_{AV} \cdot V_{d*} \tag{14}$$

Combining (13) and (14), E_{h*} can be calculated as follows:

$$E_{h*} = E_h \cdot \frac{V_{d*}}{V_d} \tag{15}$$

Following the definitions included in [67] and [68], the total daily performance ratio of the PVWPS + LIB ($PR_{PVWPS+LIB}$) is calculated in (16) as the ratio of the hydraulic energy (output energy of the PVWPS + LIB system) to the photovoltaic energy combined with the daily variation in the energy flow in the LIB (ΔE_{LIB}):

$$PR_{PVWPS+LIB} = \frac{E_h}{E_{PV} - \Delta E_{LIB}} \tag{16}$$

Since correcting the volume with the daily energy balance in the battery is equivalent to considering $\Delta E_{LIB} = 0$, the corrected total daily performance ratio of the PVWPS + LIB ($PR_{PVWPS+LIB*}$) is calculated as follows:

$$PR_{PVWPS+LIB*} = \frac{E_{h*}}{E_{PV} - \Delta E_{LIB}} = \frac{E_h \cdot \frac{V_{d*}}{V_d}}{E_{PV} - 0} = PR_{PVWPS+LIB} \cdot \frac{V_{d*}}{V_d} \tag{17}$$

A similar approach can be applied to the performance ratio of the system ($PR_{overall}$), calculated in (18) including the PV module efficiency, for obtaining in (19) the corrected performance ratio of the system ($PR_{overall*}$).

$$PR_{overall} = \frac{E_h}{H_i \cdot A_{PV} - \Delta E_{LIB}} \tag{18}$$

$$PR_{overall*} = PR_{overall} \cdot \frac{V_{d*}}{V_d} \tag{19}$$

If the energy balance in the LIB is used to correct the pumped volume, some variations in $PR_{PVWPS+LIB}$ and $PR_{overall}$ will take place, as specified in Table 5.

As might be expected, $PR_{PVWPS+LIB}$ and $PR_{overal*}$, corrected for days with radiation greater than 2 PSH, are much more uniform, as shown in Fig. 18 ($PR_{PVWPS+LIB*} = 23.84 \pm 1.69$ and $PR_{overall*} = 3.45 \pm 0.20$, expressed as Mean ± SD).

The practically horizontal trend in the relationship between these parameters and $\Delta E_{LIB}/E_{PCU\_in}$ confirms that corrections based on the energy balance (V_{d*}, $PR_{PVWPS+LIB*}$, and $PR_{overall*}$) are adequate. In addition, it is considered necessary to make these corrections to be able to compare the performance of the system between days and between operating modes. On the cloudiest days (irradiation lower than 2 PSH), the values of these parameters are considerably lower than those obtained on other days.

7. Conclusions

This paper focusses on an analysis of the operation of a high-voltage battery-based photovoltaic water pumping system, or PVWPS + LIB (HV), and aims to improve the use of solar energy. In addition, the results obtained are compared with those estimated for the equivalent direct pumping solution (DPVWPS). The facility under study constitutes a pilot plant that will later be implemented in areas with isolated and vulnerable populations. The PVWPS + LIB(HV) facility offers considerable advantages over DPWPS. The usual energy losses related to clipping at noon, or threshold irradiance levels at sunrise and sunset, can be prevented – and this energy can remain stored in the LIB and used when necessary for pumping water (or other purposes). Moreover, the inclusion of a battery avoids the disadvantages arising from quick variations in irradiance due to passing clouds, which produce many start/stop cycles that may adversely affect the motor-pump group in DPWPS. A battery enables the WPS to operate at any moment at the best motor-pump efficiency point. Efficiency is also improved if pumping coincides with sunny hours, as the system works with less energy flowing in the battery. Additionally, the use of a hybrid inverter and battery makes the selection of the VSD more flexible, since it can be chosen from the range available for conventional pump control.

The inclusion of the IoT switches enables remote control of the operation of the VSD and disconnection of the WPS if there is no pumping, thereby reducing stand-by consumption. Part of the energy provided by the LIB when the WPS is not operating can be saved if the stand-by losses in the hybrid inverter are reduced when no current is demanded in its output.

The main problem found in the PVWPS + LIB(HV) facility was related to an incorrect operation of the algorithm included in the hybrid inverter that manages the *SOC* in the battery. A low *SOC* value can cause the disconnection of the system to prevent damaging the LIB. The disconnection of the WPS prevents this occurrence, maintaining the *SOC* value needed until the LIB can be recharged.

PVWPS + LIB facilities include more components than a DPVWPS, such as the hybrid inverter and the LIB, and this involves energy losses. Consequently, the *PR* of the system decreases and so a decrease in the daily pumped volume should be expected. Nevertheless, an analysis of the data acquired for various DPVWPS operating conditions enabled identifying the best efficiency point at which the efficiency improvement in the WPS (composed of the VSD and the motor pump unit) almost compensates for the losses in the hybrid inverter and the LIB. As a result, pumped volumes in the PVWPS + LIB facility were similar to those of the estimates for the DPVWPS. Moreover, for very cloudy (rainy) days when the DPVWPS is unable to pump, it is possible to extract some water with the PVWPS + LIB, even if the *PR* values are very low compared to average values. When values of the different parameters registered with the PVWPS + LIB(HV) facility were compared with results obtained with a low-voltage LIB and a different hybrid inverter, the advantages of the new approach with respect to the extension of the pumping time and the total daily pumped volume are evident.

Although the proposed battery-based photovoltaic pumping system has higher loss factors than conventional direct photovoltaic pumping, its main advantage over the latter (in addition to those already mentioned) is that it enables basic access to electricity, which is essential for improving the quality of life in isolated regions and in humanitarian aid contexts.

The results obtained enable progress to be made in achieving the SDGs related to renewable energies, access to water and energy, sustainability, and can improve the quality of life in rural and sparsely populated areas.

Funding

This work was supported in part by the Universitat Politècnica de València (UPV - Program ADSIDEO-cooperation 2017 - project 'Characterization of sustainable systems for the pumping of water for human consumption in developing regions and/or refugee camps in Kenya through the implementation of isolated photovoltaic systems with new generation lithium-ion batteries') and in part by the International Organization for Migration under a contract entitled 'Greening humanitarian responses through enhanced Solar Energy harvesting' with funding from the Bureau for Humanitarian Assistance-USAID and Humanitarian Aid department of the European Commission (ECHO)

CRediT authorship contribution statement

José-Ángel Garrido-Sarasol: Writing – original draft, Validation, Software, Resources, Investigation, Data curation. **Salvador Orts-Grau:** Writing – original draft, Supervision, Resources, Project administration, Funding acquisition. **María Gasque:** Writing – review & editing, Writing – original draft, Visualization, Conceptualization. **Pablo González-Altozano:** Writing – review & editing, Writing – original draft, Methodology, Investigation, Formal analysis, Data curation. **Ibán Balbastre-Peralta:** Resources, Investigation, Data curation. **Francisco-José Gimeno-Sales:** Validation, Software, Resources, Investigation, Data curation, Writing – review & editing. **Salvador Segui-Chilet:** Conceptualization, Methodology, Funding acquisition, Supervision, Formal analysis, Writing – original draft, Writing – review & editing, Visualization.

Declaration of competing interest

The authors declare the following financial interests/personal relationships which may be considered as potential competing interests: Salvador Orts-Grau reports financial support was provided by International Organization for Migration. If there are other authors, they declare that they have no known competing financial interests or personal relationships that could have appeared to influence the work reported in this paper.

Data availability

The data that has been used is confidential.

Acknowledgements

To Javier Pérez, Xavier Busquets, and Monica Zheng from SolaX Power Co (https://www.solaxpower.com/), and Antonio Ramos (Technosun - https://b2b.technosun.com/) for the donation of a hybrid inverter with the corresponding high-voltage lithium battery. To Ignacio Valdeolmillos (Carlos Gavazzi company (https://automation.gavazzi.es/home - monitoring and data acquisition system) for his involvement in the project. To Sergio Ureña (Fuji Electric Europe - https://www.fujielectric-europe.com/) for his support for the project. To the Vice-Chancellor of Infrastructure at the UPV for the financial support that has enabled the project's electrical installation to be completed.

Appendix A. - compensation of the *SOC* variations in the daily pumped volume

During all the tests, it was intended that the *SOC* would be the same at the beginning and end of the day, which would facilitate establishing daily energy balances in the system, and the V_d obtained would correspond to the PV energy generated during the day. However, small daily *SOC* variations required adjusting the value of V_d.

In addition to this unavoidable effect due to the variability of photovoltaic energy, the uncontrolled variations of the *SOC* when there is no load or power generator connected to the facility must also be considered, making it necessary to correct the values of the daily pumped volume when such an event occurs. At the beginning of the day, the *SOC* was often slightly higher than the minimum value (SOC_{min}), the WPS usually stopped with *SOC* values of between 30 % and 50 % for the following reasons:

- Uncontrolled decreases/increases in *SOC* when the WPS was not in operation.
- A shutdown of the EPS output if the *SOC* decreased below 22 % (SOC_{min}).

To correct V_d with the volume variation related to the ΔSOC_{day}, denoted as ΔV_{d_LIB}, the daily variation of energy in the LIB (ΔE_{LIB}) was used to obtain the daily variation in the hydraulic energy (ΔE_{h_LIB}). Several tests were carried out to establish the relationship between ΔSOC_{day} and ΔV_{d_LIB}. Fig. A1 shows the most important magnitudes in the PVWPS + LIB(HV) facility during a test in which the WPS was in operation with $f_{VSD} = 37$ Hz and the PV array was disconnected ($P_{PV} = 0$ W). The values considered in the LIB discharging test are detailed in Table A1, where the active power in the EPS output (P_{EPS}) provided by the hybrid inverter ($P_{EPS} = 1605$ W) was corrected to 924 W, as calculated in (4).

An analysis of the collected data shows that the variation of the *SOC* during the test was equal to 59 % ($\Delta SOC_{test} = 96\ \% - 37\ \%$). The test duration ($\Delta t_{test}$) was 190 min (equivalent to $3.1\widehat{6}$ h), with an LIB discharge that presented a constant power behavior ($P_{LIB} = $ const.), with a small decrease in the operating voltage ($\Delta V_{LIB} = -7$ V, equivalent to –2.94 % of the test initial conditions) that was compensated by a small increase in the LIB current ($\Delta I_{LIB} = +0.05$ A, equivalent to + 1.12 % of the initial test conditions). This test was similar to that presented in [36], although the results differ slightly because the LIB output power was not constant during the pumping interval, varying from 530 W to 385.6 W, with a variation of –20 % in the current and –9 % in the voltage. The good behavior of the LIB during the discharge test shows the correct operation of the battery management system (BMS) that controls its operations. However, some details are pending adjustment – among them, the *SOC* variation that was equal to 28.7 % if the total discharged energy of 3.3 kWh was compared with the nominal capacity of 11.5 kWh, which did not match the value of 59 % obtained from the data provided by the hybrid inverter monitoring system. This discrepancy could be caused by the hybrid inverter controller, which did not correctly consider that two stacks of battery were connected in series, and so made the *SOC* calculations as if only one stack was connected. Thus, for just one stack with 5.8 kWh of capacity, the discharge of 3.3 kWh would represent a $\Delta SOC = -56.8$ %, and this figure is very close to the value of 59 % provided by the hybrid inverter.

The total pumped volume during the test (ΔV_{test}) is calculated as follows:

$$\Delta V_{test} = 190\,\text{min} \cdot 1.5 \frac{\text{L}}{\text{s}} \cdot \frac{60\text{s}}{1\,\text{min}} = 17100\,\text{L} = 17.1\,m^3 \tag{A1}$$

The obtained values yield to the following correction of the pumped volume considering the daily *SOC* variation ($\Delta V_{d^*\_LIB\_SOC}$ in m^3/d), calculated using the data collected by the monitoring system:

$$\Delta V_{d^*\_LIB\_SOC} = \frac{\Delta V_{test}}{\Delta SOC_{test}} \cdot \Delta SOC_{day} = \frac{17.1\, m^3}{59\,\%} \cdot \Delta SOC_{day} = 0.28983 \cdot \Delta SOC_{day} \left(m^3/d\right) \quad \text{(A2)}$$

Appendix B. – Estimation of the daily pumped volume with the equivalent direct PV pumping solution

Four approaches were used to estimate the total volume pumped for every day that the direct-solution could have pumped ($V_{d\_DPVWPS\_est*}$). The expressions were obtained from the analysis of 47 days operating in the DPVWPS mode, including days with different *GI* profiles and considering *GI* in W/m^2. The conditions used to obtain the different approaches, mathematical equations of the fourth models, and values of their respective goodness-of-fit coefficients (coefficients of determination r^2) are the following:

- Estimation 1 ($V_{d\_DPVWPS\_est1}$) was obtained by applying (B1), estimating in (B2) the flow rate until midday while considering $GI_{thre} = GI_{thre\_start} =$ 310 W/m^2 and using (B3) from midday to midnight with $GI_{thre} = GI_{thre\_stop} =$ 250 W/m^2. The expressions were obtained considering only sunny days.

$$V_{d\ DPVWPS\ est1\ DOY^*} = \sum\nolimits_k V_{d,k} = t_k \left(\sum\nolimits_k Q_{k00:00\to11:59} + \sum\nolimits_k Q_{k12:00\to23:59} \right) \quad \text{(B1)}$$

$$Q_{k\ 00:00\to11:59}(L/s) = -2.5568 \cdot GI_k^2 + 5.4688967 \cdot GI_k - 0.3950132302 \qquad r^2 = 0.9873 \quad \text{(B2)}$$

$$Q_{k\ 12:00\to23:59}(L/s) = -2.4249 \cdot GI_k^2 + 4.7903241 \cdot GI_k + 0.1271494163 \qquad r^2 = 0.9905 \quad \text{(B3)}$$

- Estimation 2: use the fitting analysis shown in Fig. 12 in [20], where Q_k is obtained without cloudy days in the fitting analysis, with the values of *GI* in W/m^2, and considering the following *GI* threshold values: $GI_{thre\_start} =$ 301.30 W/m^2 and $GI_{thre\_stop} =$ 208.90 W/m^2.

$$V_{d\ DPVWPS\ est2\ DOY^*} = t_k \sum\nolimits_k \left(-2.3379 \cdot GI_k^2 + 4.9183 \cdot GI_k - 0.0662 \right) \qquad r^2 = 0.9428 \quad \text{(B4)}$$

- Estimation 3 ($V_{d\_DPVWPS\_est3}$) is equivalent to Estimation 1, but considering all the days of operation of the DPVWPS (sunny and cloudy days) and $GI_{thre\_start} = GI_{thre\_stop} =$ 330 W/m^2.

$$V_{d\ DPVWPS\ est3\ DOY^*} = t_k \sum\nolimits_k \left(-2.1389 \cdot GI_k^2 + 4.7289585 \cdot GI_k - 0.1219153831 \right) \qquad r^2 = 0.5514 \quad \text{(B5)}$$

- Estimation 4: uses the fitting analysis detailed in Fig. 3 in [20] and considers $GI_{thre} = GI_{thre\_start} =$ 301.30 W/m^2:

$$V_{d\ DPVWPS\ est4\ DOY^*} = 11.923 \cdot PSH - 6.7705 \qquad r^2 = 0.9580 \quad \text{(B6)}$$

The volume pumped with the DPVWPS was estimated using these four approaches throughout the present work.

References

[1] Rahman MM, Khan I, Field DL, Techato K, Alameh K. Powering agriculture: Present status, future potential, and challenges of renewable energy applications. Renew Energy 2022;188:731–49. https://doi.org/10.1016/j.renene.2022.02.065.

[2] United Nations - Dept. of Economic and Social Affairs. (2015). Sustainable Development Goals, from https://sustainabledevelopment.un.org/sdgs, accessed 23-2-2020.

[3] Foster, R.; Ghassemi, M.; Cota, A. (2009). *Solar Energy: Renewable Energy and the Environment*, *Solar Energy: Renewable Energy and the Environment*, CRC Press. doi: 10.5860/choice.47-5672.

[4] Baranda Alonso J, Sandwell P, Nelson J. The potential for solar-diesel hybrid mini-grids in refugee camps: a case study of Nyabiheke camp Rwanda. Sustainable Energy Technol Assessments 2021;44:1–18. https://doi.org/10.1016/j.seta.2021.101095.

[5] Ki-moon, B.; Secretary General, U. (2011). The Human Right to Water and Sanitation, 8, from https://www.un.org/waterforlifedecade/pdf/human_right_to_water_and_sanitation_media_brief.pdf, accessed 2-1-2022.

[6] García R, Naves A, Anta J, Ron M, Molinero J. Drinking water provision and quality at the Sahrawi refugee camps in Tindouf (Algeria) from 2006 to 2016. Sci Total Environ 2021;780:1–15. https://doi.org/10.1016/j.scitotenv.2021.146504.

[7] World Health Organization. (n.d.). Water Sanitation and Health: humanitarian emergencies, from https://www.who.int/teams/environment-climate-change-and-health/water-sanitation-and-health/environmental-health-in-emergencies/humanitarian-emergencies, accessed 2-1-2023.

[8] Ossenbrink, J.; Pizzorni, P.; van der Plas, T. (2018). Solar PV systems for refugee camps. A quantitative and qualitative assessment of drivers and barriers, 1–9, from https://ethz.ch/content/dam/ethz/special-interest/mtec/mtec-department-dam/news/files/solar-pv-in-refugee-camps, accessed 30-3-2023.

[9] Muralidhar K, Rajasekar N. A review of various components of solar water-pumping system: Configuration, characteristics, and performance. Int Trans Electrical Energy Sys 2021;31(9):1–33. https://doi.org/10.1002/2050-7038.13002.

[10] Betka A, Attali A. Optimization of a photovoltaic pumping system based on the optimal control theory. Sol Energy 2010;84(7):1273–83. https://doi.org/10.1016/j.solener.2010.04.004.

[11] Elkholy MM, Fathy A. Optimization of a PV fed water pumping system without storage based on teaching-learning-based optimization algorithm and artificial neural network. Sol Energy 2016;139:199–212. https://doi.org/10.1016/j.solener.2016.09.022.

[12] Errouha M, Derouich A, Nahid-Mobarakeh B, Motahhir S, El Ghzizal A. Improvement control of photovoltaic based water pumping system without energy storage. Sol Energy 2019;190:319–28. https://doi.org/10.1016/j.solener.2019.08.024.

[13] Calero-Lara M, López-Luque R, Casares FJ. Methodological advances in the design of photovoltaic irrigation. Agronomy 2021;11:1–27. https://doi.org/10.3390/agronomy11112313.

[14] Allouhi A, Buker MS, El-houari H, Boharb A, Benzakour Amine M, Kousksou T, et al. PV water pumping systems for domestic uses in remote areas: Sizing process, simulation and economic evaluation. Renew Energy 2019;132:798–812. https://doi.org/10.1016/j.renene.2018.08.019.

[15] Soenen C, Reinbold V, Meunier S, Cherni JA, Darga A, Dessante P, et al. Comparison of tank and battery storages for photovoltaic water pumping. Energies 2021;14:1–16. https://doi.org/10.3390/en14092483.

[16] Jahanfar, A.; Iqbal, M. T. (2022). An Optimum Sizing for a Hybrid Storage System in Solar Water Pumping Using ICA, *2022 IEEE International IOT, Electronics and Mechatronics Conference, IEMTRONICS 2022*, Institute of Electrical and Electronics Engineers Inc., 1–6. doi:10.1109/IEMTRONICS55184.2022.9795848.

[17] Naval N, Yusta JM. Comparative assessment of different solar tracking systems in the optimal management of PV-operated pumping stations. Renew Energy 2022;200:931–41. https://doi.org/10.1016/J.RENENE.2022.10.007.

[18] Odeh I, Yohanis YG, Norton B. Economic viability of photovoltaic water pumping systems. Sol Energy 2006;80(7):850–60. https://doi.org/10.1016/j.solener.2005.05.008.

[19] Zamanlou M, Iqbal MT. Design and Analysis of Solar Water Pumping with Storage for Irrigation in Iran. In: IEEE 17th International Conference on Smart Communities: Improving Quality of Life Using ICT, IoT and AI; 2020. p. 118–24. https://doi.org/10.1109/HONET50430.2020.9322660.

[20] Orts-Grau S, Gonzalez-Altozano P, Gimeno-Sales FJ, Balbastre-Peralta I, Marquez CIM, Gasque M, et al. Photovoltaic water pumping: comparison between direct and lithium battery solutions. IEEE Access 2021;9:1–5. https://doi.org/10.1109/ACCESS.2021.3097246.

[21] Gasque M, Gonzalez-Altozano P, Gimeno-Sales FJ, Orts-Grau S, Balbastre-Peralta I, Martinez-Navarro G, et al. Energy Efficiency Optimization in Battery-Based Photovoltaic Pumping Schemes. IEEE Access 2022;10:54064–78. https://doi.org/10.1109/ACCESS.2022.3175586.

[22] Sena dos Santos W, Ferreira Torres P, Ubaiara Brito A, Arrifano Manito AR, Figueiredo Pinto Filho G, Leão Monteiro W, Negrão Macêdo W. A novel method to determine the optimal operating point for centrifugal pumps applied in photovoltaic pumping systems. Sol Energy 2021;221:46–59. https://doi.org/10.1016/j.solener.2021.04.005.

[23] Gualteros S, Rousse DR. Solar water pumping systems: a tool to assist in sizing and optimization. Sol Energy 2021;225:382–98. https://doi.org/10.1016/j.solener.2021.06.053.

[24] Chandel SS, Nagaraju Naik M, Chandel R. Review of solar photovoltaic water pumping system technology for irrigation and community drinking water supplies. Renew Sustain Energy Rev 2015;49:1084–99. https://doi.org/10.1016/j.rser.2015.04.083.

[25] Periasamy P, Jain NK, Singh IP. A review on development of photovoltaic water pumping system. Renew Sustain Energy Rev 2015;43:918–25. https://doi.org/10.1016/j.rser.2014.11.019.

[26] Sontake VC, Kalamkar VR. Solar photovoltaic water pumping system - a comprehensive review. Renew Sustain Energy Rev 2016;59:1038–67. https://doi.org/10.1016/j.rser.2016.01.021.

[27] Muhsen DH, Khatib T, Nagi F. A review of photovoltaic water pumping system designing methods, control strategies and field performance. Renew Sustain Energy Rev 2017;68:70–86. https://doi.org/10.1016/j.rser.2016.09.129.

[28] Aliyu M, Hassan G, Said SA, Siddiqui MU, Alawami AT, Elamin IM. A review of solar-powered water pumping systems. Renew Sustain Energy Rev 2018;87:61–76. https://doi.org/10.1016/j.rser.2018.02.010.

[29] Poompavai T, Kowsalya M. Control and energy management strategies applied for solar photovoltaic and wind energy fed water pumping system: a review. Renew Sustain Energy Rev 2019;107:108–22. https://doi.org/10.1016/j.rser.2019.02.023.

[30] Shepovalov OV, Belenov AT, Chirkov SV. Review of photovoltaic water pumping system research. Energy Rep 2020;6:306–24. https://doi.org/10.1016/j.egyr.2020.08.053.

[31] W. Kiprono, A.; Ibáñez Llario, A. (2020). *Solar Pumping for Water Supply: Harnessing Solar Power in Humanitarian and Development*, (Practical Action Publishing, Ed.) *Solar Pumping for Water Supply* (1st. ed.), Practical Action Publishing, Rugby, UK. doi:10.3362/9781780447810.

[32] Verma, S.; Mishra, S.; Chowdhury, S.; Gaur, A.; Mohapatra, S.; Soni, A.; Verma, P. (2020). Solar PV powered water pumping system - A review, *Materials Today: Proceedings* (Vol. 46), Elsevier Ltd, 5601–5606. doi:10.1016/j.matpr.2020.09.434.

[33] Singh, D. B.; Mahajan, A.; Devli, D.; Bharti, K.; Kandari, S.; Mittal, G. (2020). A mini review on solar energy based pumping system for irrigation, *Materials Today: Proceedings* (Vol. 43), Elsevier Ltd, 417–425. doi:10.1016/j.matpr.2020.11.716.

[34] Gevorkov L, Domínguez-García JL, Romero LT. review on solar photovoltaic-powered pumping systems. Energies 2023;16(1):1–21. https://doi.org/10.3390/en16010094.

[35] Harkness B, Guthrie P, Burt M. Sustainable water pumping in refugee camps: solar PV / diesel hybrid scenarios at Nyarugusu Tanzania. 40th WEDC Int. Conf. 2017: 1–7.

[36] World Bank Group. (2014). Solar irrigation with electric vehicle : public-private approach to energy, water and food nexus, *Washington, D.C*, 1–58, from http://documents.worldbank.org/curated/en/825921468142177741/Solar-irrigation-with-electric-vehicle-public-private-approach-to-energy-water-and-food-nexus, accessed 20-5-2017.

[37] Martinez-Laserna E, Gandiaga I, Sarasketa-Zabala E, Badeda J, Stroe DI, Swierczynski M, et al. Battery second life: hype, hope or reality? a critical review of the state of the art. Renewable Sustainable Energy Rev. 2018;93:701–18. https://doi.org/10.1016/j.rser.2018.04.035.

[38] Zhu J, Mathews I, Ren D, Li W, Cogswell D, Xing B, et al. End-of-life or second-life options for retired electric vehicle batteries. Cell Reports Phys. Sci. 2021;2(8): 1–26. https://doi.org/10.1016/J.XCRP.2021.100537.

[39] Falk J, Nedjalkov A, Angelmahr M, Schade W. Applying lithium-ion second life batteries for off-grid solar powered system—a socio-economic case study for rural development. Zeitschrift Für Energiewirtschaft 2020;44(1):47–60. https://doi.org/10.1007/s12398-020-00273-x.

[40] Bhayo BA, Al-Kayiem HH, Gilani SI. Assessment of standalone solar PV-Battery system for electricity generation and utilization of excess power for water pumping. Sol Energy 2019;194:766–76. https://doi.org/10.1016/j.solener.2019.11.026.

[41] Cacciato, M.; Finocchiaro, L.; Nobile, G.; Scarcella, G.; Scelba, G. (2016). Assessment of energy management strategies for battery assisted solar pumping systems, *2016 International Symposium on Power Electronics, Electrical Drives, Automation and Motion, SPEEDAM 2016*, Institute of Electrical and Electronics Engineers Inc., 575–581. doi:10.1109/SPEEDAM.2016.7526000.

[42] Herraiz JI, Fernández-Ramos J, Hogan Almeida R, Báguena EM, Castillo-Cagigal M, Narvarte L. On the tuning and performance of stand-alone large-power PV irrigation systems. Energy Conversion Management: X 2022;13:1–16. https://doi.org/10.1016/j.ecmx.2021.100175.

[43] Bhatia, M.; Angelou, N. (2015). Beyond Connections: Energy Access Redefined, *ESMAP Technical Report*, ESMAP Technical Report, 1–244, from http://hdl.handle.net/10986/24368, accessed 23-5-2023.

[44] Harkness B, Guthrie P, Burt M. Sustainable water pumping in refugee camps: costs and benefits of over-sized solar PV systems. In: 40th WEDC International Conference; 2017. p. 1–7.

[45] Fuentes M, Vivar M, Hosein H, Aguilera J, Muñoz-Cerón E. Lessons learned from the field analysis of PV installations in the Saharawi refugee camps after 10 years of operation. Renew Sustain Energy Rev 2018;93:100–9. https://doi.org/10.1016/j.rser.2018.05.019.

[46] Neves D, Baptista P, Pires JM. Sustainable and inclusive energy solutions in refugee camps: developing a modelling approach for energy demand and alternative renewable power supply. J Clean Prod 2021;298:1–15. https://doi.org/10.1016/j.jclepro.2021.126745.

[47] International Renewable Energy Agency. (2019). *Renewables for refugee settlements: Sustainable energy access in humanitarian situations*.

[48] Diouf B, Pode R. Potential of lithium-ion batteries in renewable energy. Renew Energy 2015;76:375–80. https://doi.org/10.1016/j.renene.2014.11.058.

[49] Amirante R, Cassone E, Distaso E, Tamburrano P. Overview on recent developments in energy storage: Mechanical, electrochemical and hydrogen technologies. Energ Conver Manage 2017;132:372–87. https://doi.org/10.1016/j.enconman.2016.11.046.

[50] Zubi G, Dufo-López R, Carvalho M, Pasaoglu G. The lithium-ion battery: State of the art and future perspectives. Renew Sustain Energy Rev 2018;89:292–308. https://doi.org/10.1016/j.rser.2018.03.002.

[51] Paredes-Sánchez JP, Villicaña-Ortíz E, Xiberta-Bernat J. Solar water pumping system for water mining environmental control in a slate mine of Spain. J Clean Prod 2015;87:501–4. https://doi.org/10.1016/j.jclepro.2014.10.047.

[52] Kalla UK, Rajawat SPS, Singh S, Bhati N. Solar PV fed Battery Powered PMBLDCM driven Water Pumping System using Cuk Converter. In: Proceedings of 2021 IEEE 2nd International Conference on Smart Technologies for Power, Energy and Control; 2021. https://doi.org/10.1109/STPEC52385.2021.9718691.

[53] Ashraf U, Iqbal MT. Optimised design and analysis of solar water pumping systems for pakistani conditions. Energy Power Eng 2020;12(10):521–42. https://doi.org/10.4236/epe.2020.1210032.

[54] Sharma A, Gupta TN. Solar-powered PMSM-driven battery-supported water pumping system. Lecture Notes Electrical Eng. 2022;817:117–28. https://doi.org/10.1007/978-981-16-7393-1_10.

[55] Shukla S, Singh B, Shaw P, Al-Durra A, El-Fouly THM, El-Saadany EF. A new analytical mppt-based induction motor drive for solar PV water pumping system with battery backup. IEEE Trans Ind Electron 2022;69:6. https://doi.org/10.1109/TIE.2021.3091929.

[56] Parveen H, Sharma U, Singh B. Battery supported solar water pumping system with adaptive feed-forward current estimation. IEEE Trans Energy Convers 2022;37:3. https://doi.org/10.1109/TEC.2022.3147496.

[57] Mishra AK, Singh B, Kim T. An efficient and credible grid-interfaced solar pv water pumping system with energy storage. IEEE J Photovoltaics 2022;12:3. https://doi.org/10.1109/JPHOTOV.2022.3147449.

[58] Solax Power Network Technology Ltd. (2021). Solax X1-Hybrid User Manual, 2, from https://www.solaxpower.com/wp-content/uploads/2021/02/X1-hybrid-1.pdf, accessed 9-3-2022.

[59] Solax Power Network Technology Ltd. (2022). Solax X3-hybrid G4 datasheet, 2, from www.solaxpower.com, accessed 6-9-2022.

[60] Goodwe. (2022). GoodWe GW_ET Plus three phase hybrid inverter datasheet, 2, from https://en.goodwe.com/et-plus-series-three-phase-hybrid-solar-inverter, accessed 21-8-2022.

[61] Megarevo. (2021). Megarevo three phase hybrid inverter, 2, from https://www.megarevopower.com/productinfo3.html, accessed 18-8-2022.

[62] Gimeno-Sales FJ, Orts-Grau S, Escribá-Aparisi A, González-Altozano P, Balbastre-Peralta I, Martínez-Márquez CI, et al. PV monitoring system for a water pumping scheme with a lithium-ion battery using free open-source software and iot technologies. Sustainability (switzerland) 2020;12(24):1–28. https://doi.org/10.3390/su122410651.

[63] Solax Power Network Technology Ltd. (2020). Solax Triple Power Lithium-ion Battery User Manual 50Ah, 22, from https://www.solaxpower.com/wp-content/uploads/2020/02/Triple-Power-T58_user-manual-1.pdf, accessed 9-3-2022.

[64] Aideepen. (2023). Modbus RTU 2 channel Relay Module 485 TTL Communication, from https://www.aideepen.com/collections/relay/products/1pcs-modbus-rtu-1-2-4-8-channel-relay-module-485-ttl-communication-1-2-4-8-channel-input-relay-module-12v?variant=31547150893108, accessed 16-5-2023.
[65] Fotek. (2013). Solid state module, from https://www.fotek.com.tw/en-gb/product-category/143, accessed 16-5-2023.
[66] González I, Calderón AJ, Folgado FJ. IoT real time system for monitoring lithium-ion battery long-term operation in microgrids. J Storage Mater 2022;51:1–16. https://doi.org/10.1016/J.EST.2022.104596.
[67] Sontake VC, Tiwari AK, Kalamkar VR. Experimental investigations on the seasonal performance variations of directly coupled solar photovoltaic water pumping system using centrifugal pump. Environ Dev Sustain 2021;23(6):8288–306. https://doi.org/10.1007/s10668-020-00965-x.
[68] Sontake VC, Tiwari AK, Kalamkar VR. Performance investigations of solar photovoltaic water pumping system using centrifugal deep well pump. Therm Sci 2020;24:2915–27. https://doi.org/10.2298/TSCI180804282S.